



## Research paper

# Multi-objective multi-path COVID-19 medical waste collection problem with type-2 fuzzy logic based risk using partial opposition-based weighted genetic algorithm



Somnath Maji <sup>a</sup>\*, Samir Maity <sup>b</sup>, Debasis Giri <sup>c</sup>, Izabela Nielsen <sup>b</sup>, Manoranjan Maiti <sup>d</sup>

<sup>a</sup> Department of Computer Science & Engineering, Maulana Abul Kalam Azad University of Technology, Nadia 741249, West Bengal, India

<sup>b</sup> Operations Research Group, Department of Materials and Production, Aalborg University, 9220, Aalborg, Denmark

<sup>c</sup> Department of Information Technology, Maulana Abul Kalam Azad University of Technology, Nadia 741249, West Bengal, India

<sup>d</sup> Department of Mathematics, Vidyasagar University, Midnapur 721102, West Bengal, India

## ARTICLE INFO

**Keywords:**

Medical waste  
Collection problem  
Occupational risk  
Genetic algorithm  
Type-2 fuzzy logic

## ABSTRACT

The transportation and handling of the most infectious coronavirus disease 2019 (COVID-19) waste are vital from the point of view of risk and safety. Here, a multi-objective, multi-path medical waste collection routing problem with occupational and transportation risks is considered. A specially equipped medical collection van with appropriately dressed collectors starts from a dumping campus and returns to it for disposal after collecting the COVID-19 hazardous wastes from rural medical centers/hospitals. Transportation, fixed charge, and loading costs are considered in this system. The occupational risk in each medical center depends on the number of workers involved, the collected amount of hazardous waste, and the storage period. The transportation risk depends on the probability of an accident which is determined by Type-1 and Type-2 fuzzy logic, the environmental condition of the accident, the length of the route, the weight of carried waste, and the population around the accident site which are the key applications of artificial intelligence. Here, the objective is to minimize the total cost, occupational, and transportation risks. This multi-objective problem is converted to a single-objective one through the weighted sum method. To solve it, we develop and implement a genetic algorithm with partial opposition-based learning-dependent initialization and mutation, probabilistic selection, and weightage-based comparison crossover. The proposed algorithm is tested against some standard benchmark instances, its effectiveness is shown through statistical tests and performance metrics. From the numerical experiments, it is observed that total cost is inversely related to both risks, but their behavior is non-linear. Some managerial insights are presented.

## 1. Introduction and motivation

Medical waste includes potentially harmful bacteria infecting hospital patients, personnel, the general public, and the environment. For the last two years, the coronavirus (COVID-19) pandemic has created several problems in society, including waste disposal. It has generated huge infectious waste (Tsai, 2021) of different types. Handling this waste at the health centers in developing countries is a difficult task due to several reasons, such as lack of awareness, training, and seriousness, huge population, insufficient resources, including protective materials, etc. It is not only the colossal waste amount, its highly infectious nature is the main problem. During the transportation of waste, the accident of transporting vehicles is very dangerous because it affects people, living beings, and the environment around the place of the accident. Thus,

the storage of medical waste in healthcare facilities and the transfer of these potentially hazardous items to the treatment facilities through proper roads, areas, etc., are difficult jobs that are interdependent (presented in Fig. 1) (Taslimi et al., 2020). Therefore, this problem demands investigation.

Due to the rapid development of infrastructure throughout the world, more than one path is available for transportation between two arbitrary medical centers. Governments in developing countries like- India, Sri Lanka, etc., have constructed several “National Highways” that connect various cities and collect “toll taxes”, called fixed charge (Hirsch and Dantzig, 1968) from the passing vehicles for maintenance of the roads. In spite of these, some of these roads are very bad and congested, which leads to accidents often.

\* Corresponding author.

E-mail addresses: [somnathmajivucs@gmail.com](mailto:somnathmajivucs@gmail.com) (S. Maji), [samirm@mp.aau.dk](mailto:samirm@mp.aau.dk) (S. Maity), [debasis\\_giri@hotmail.com](mailto:debasis_giri@hotmail.com) (D. Giri), [izabela@mp.aau.dk](mailto:izabela@mp.aau.dk) (I. Nielsen), [mmaiti2005@yahoo.co.in](mailto:mmaiti2005@yahoo.co.in) (M. Maiti).

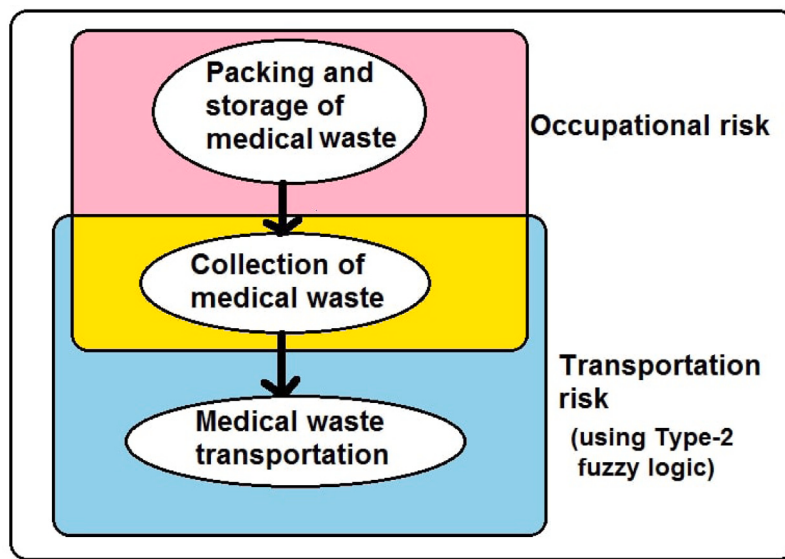


Fig. 1. Graphical representation of two risks.

In the system of bringing the medical waste to the dumping ground from different rural health centers, several questions arise. These are (i) As there are several rural hospitals connected through different routes among themselves and the dumping ground, what should be the suitable routing plan along with the appropriate paths to achieve the specified objectives? (ii) This waste collection process involves occupational and environmental risks along with transportation costs, what should be the collection plan so that both risks and transportation costs are minimized? (iii) Transportation risk, in this case, is mainly due to an accident that spreads infections in the area of the accident. The probability of accidents depends on the condition of the road's surface roughness and congestion, which are defined imprecisely by words like 'very bad', and 'crowded often', etc. Thus, how do express the accident probability with the above imprecise verbal words?

Keeping the above facts in mind in this investigation, we consider that a specially equipped medical vehicle with properly dressed collectors moves from a waste disposal center, collects the hazardous waste from different rural health centers/hospitals, and comes back to the dumping campus. The questions that prompted from this context are answered. The probability of an accident is expressed in terms of road conditions and congestion through Type-2 fuzzy logic. Here, the objective is to find a suitable routing plan through the appropriate paths so that occupational and transportation risks and total costs are minimal.

To solve the above multi-objective NP-hard problem, we develop a partial opposition-based genetic algorithm (POBGA) with partial opposition-based learning (POBL) dependent initialization and mutation, probabilistic selection, and problem-specific weighted crossover. To maintain the diversity in the solution space and to get a feasible solution, POBL takes a vital role. Till now, mainly POBL is used in the continuous optimization problem. In this discrete routing problem, POBL is used in initialization and mutation.

The multi-objective, multi-path COVID-19 medical waste collection problem (MOMPC-19MWC) consists of four models-minimization of transportation risk (Model A), occupational risk (Model B), total cost (Model C), and all the above objectives (Model D). The overview of the present investigation is given in Fig. 3. It is illustrated through real-life medical waste management problems in Bankura district, West Bengal, India, and the obtained results were analyzed.

Novelties in this investigation are as follows:

- MOMPC-19MWC is formulated as transportation (due to accident), occupational risks (during handling), and total cost minimization problem

- The probability of an accident is expressed using Type-2 fuzzy logic based on road congestion and surface structure
- Partial OBL-based initialization and mutation are introduced in POBGA
- Probabilistic selection and problem-specific weighted crossover are also considered
- Friedman's test, Post-hoc paired comparisons, and performance metrics are studied to validate the proposed algorithm
- MOMPC-19MWC problems are solved by POBGA using the weighted sum method

The paper is arranged as follows: In Section 1, a concise introduction and motivation are presented. A brief literature review is given in the Section 2. Section 3 gives details of the model. Section 4 studies the solutions methodology. Validation of the proposed algorithm is presented in 5. Numerical experiments of proposed models are included in Section 6. In Section 7, a brief discussion is given. Managerial insights are presented in Section 8. Finally, the conclusion, limitations, and future scope are available in Section 9.

## 2. Literature review

There have been many investigations done for medical waste routing problems. Jingwei and Zujun (2010) designed a multi-period location-routing-inventory problem with a fuzzy volume of recyclable medical waste. A two-phase heuristic algorithm was also suggested for solving the problem. Nolz et al. (2011) formulated a collector-managed inventory routing problem. They developed a tabu search-based algorithm to optimize the selection of visit dates and associated vehicle routes. Moustafa et al. (2013) investigated large-scale vehicle routing problems for waste collection in Alexandria, Egypt. They developed a geographic information system (GIS)-based model and solved it through *TransCAD*<sup>®</sup>. Another work by He and Liu (2015), studied a vehicle routing problem (VRP) with balance constraints considering expenses and transportation risk through GA. They used reverse evaluation operations in GA. He et al. (2016) focused on the reverse logistics activity of medical waste collection in China. The policy and regulations, processing technology, classification, packaging, etc., are solved through network optimization. An environmental and human health risks posed by the procedures used to handle medical waste currently in use in hospitals in Sana'a, Yemen, according to Alwabri et al. (2017). The current treatment of medical waste in the hospitals under study involved several actions and processes, all of which were

**Table 1**  
Literature survey.

References (year wise)	Medical waste	COVID Medical waste	Multi-path	Transportation risk	Occupational risk	Type-2 fuzzy logic	Fixed cost	Single objective	Multi-objective	Exact	Heuristic	OBI concept	Weighted crossover
Jingwei and Zujun (2010)	✓							✓	✓		✓		
Nolz et al. (2011)	✓	✓						✓	✓		✓		
Güvez et al. (2012)	✓	✓						✓	✓		✓		
Moustafa et al. (2013)	✓							✓	✓		✓		
Nolz et al. (2014)	✓							✓	✓		✓		
He and Liu (2015)	✓							✓	✓				
He et al. (2016)	✓							✓	✓		✓		
Alwabri et al. (2017)	✓							✓	✓		✓		
Hajar et al. (2018)	✓							✓	✓		✓		
Mete and Serin (2019)	✓							✓	✓		✓		
Liu et al. (2020)	✓		✓					✓	✓		✓		
Taslimi et al. (2020)	✓								✓		✓		
Yu et al. (2020)	✓		✓						✓		✓		
Eren and Tuzkaya (2021)	✓		✓						✓		✓		
Tirkolaee et al. (2021)	✓		✓						✓		✓		
Govindan et al. (2021)	✓		✓						✓		✓		
Li et al. (2022)	✓		✓						✓		✓		
Rubab et al. (2022)	✓		✓										
Present investigation	✓	✓	✓	✓	✓	✓	✓	✓	✓	✓	✓	✓	✓

analyzed using the preliminary risk analysis technique. Hajar et al. (2018) focused on on-site medical waste multi-objective VRP with time windows. They considered to minimized the time and risk to the patients, hospital staff, visitors, and the surrounding environment, and solved it through CPLEX solver. Mete and Serin (2019) studied the optimization of the medical waste routing problem, the case of the TRB1 region in Turkey. They minimized the risk and total distance using GIS solution approach.

Recently, some researchers studied the COVID medical waste routing (Tirkolaee et al., 2021; Tang et al., 2023; Kulkarni and Anantharama, 2020; Olatayo et al., 2021; Das et al., 2021; Kargar et al., 2020; Mosallanezhad et al., 2023). Liu et al. (2020) investigated COVID-19 medical waste transportation using Ant colony optimization. They used the Q-value method to allocate medical waste vehicles. Again, reverse logistics network design for medical waste in Wuhan (China) was investigated by Yu et al. (2020). They solved multi-objectives (risk and cost) through an interactive, fuzzy approach. Tirkolaee et al. (2021) studied the sustainability of the location-routing problem during the pandemic situation using a fuzzy chance-constrained programming technique (to address the uncertainty). They implemented a weighted goal programming method to deal with the multi-objective problem. Govindan et al. (2021) focused on a bi-objective mixed integer linear programming (MILP) model for COVID medical waste. They solved the location-routing problem to minimize the total costs and risk through goal programming. Li et al. (2022) investigated minimizing collection and transportation links to reduce municipal solid waste risks in China. Rubab et al. (2022) focused on an AI-based medical waste management strategy. They used AI/ML (genetic algorithms, artificial neural networks) classification and disposal of COVID-19 waste for effective medical waste management.

COVID-19 medical waste collection is a crucial challenge (Nabavi-Peleesarai et al., 2022; Mahyari et al., 2022; Al-Omran et al., 2021). Several researchers investigated different COVID-19 situations. Eren and Tuzkaya (2021) investigated the safety and distance of transporting COVID-19 medical wastes, and the problem was formulated through VRP. They used safety scores for the safest and shortest transportation routes for medical waste vehicles. Again, Taslimi et al. (2020) focused on transportation and storage risk-based medical waste collection and routing. In this investigation, only one route connecting the medical

centers and dumping grounds was considered. The effect of road surface and congestion on the accident was not taken into account. They used CPLEX for routing problem and presented a case study. A concise literature review is presented in Table 1.

In routing problems (Shang et al., 2023; Oladzad-Abbasabady et al., 2023; Fuertes et al., 2023; Maji et al., 2023a; Ergün et al., 2023; Maji et al., 2023c), different types of fixed charges are considered. When a vehicle passes through a location to transfer goods from a source to a destination, a fixed cost, i.e., the toll tax at the toll plaza, is collected. Fixed cost for vehicle operation are investigated by Choi and Lee (2011). Another type of fixed cost is considered by Voß (1996), where the fixed cost is incurred by visiting new markets. The present research work incorporates fixed charge costs in terms of toll tax among two arbitrary centers.

In solving multi-objective problems, several approaches are available in the literature (Peng et al., 2022; Wan et al., 2023; Tam et al., 2022; Zhou and Bian, 2022). In this investigation, using the weighted sum method (Kim and De Weck, 2006), we have solved the multi-objective problem.

Since GA is a well-known meta-heuristic method for tackling combinatorial optimization problems, we use a variation of GA to solve the suggested MOMPC-19MWCP. To maintain the diversity of solutions spaces, we introduce partial opposition-based learning in GA. Here, two chromosomes are generated from a single one using the OBI concept. These types of POBL are introduced in discrete optimization. In continuous optimization, POBL is used by several researchers (Si et al., 2022; Xu et al., 2021, etc.). Our study mandates partial OB for both the initialization and mutation processes. Different types of crossover (cf. Kohestani, 2020; Maji et al., 2024; Gupta, 2022; Koc et al., 2022; Maji et al., 2023b; Saxena, 2019, etc.) are performed in GA in various problems. This study introduces a problem-specific weighted crossover for better performance.

### 3. Proposed multi-path medical waste collection problem

#### 3.1. Notations

Notation and corresponding descriptions are presented in Table 2

**Table 2**

Notation and description of parameters and decision variables.

Notation	Description
Sets:	
$N$	Number of nodes (1, 2, 3, ..., $N$ ),
$i, j, k$	Index set,
$Q$	Set of nodes {1, 2, 3, ..., $N$ }, $N = 1$ is depot,
$R_{i,i+1}$	All paths between $i$ th node to $(i+1)$ th node.
Parameters:	
$r_{i,i+1}$	Random path within $R_{i,i+1}$ ,
$x_i$	$i$ th visiting center,
$\rho(x_i, x_{i+1}, r_{i,i+1})$	Accident probability per unit length from $i$ th to $(i+1)$ th node using $r_{i,i+1} \in R_{i,i+1}$ route,
$\alpha(x_i, x_{i+1}, r_{i,i+1})$	Consequence of hazardous waste exposure to people for an accident happening from $i$ th center to $(i+1)$ th center using $r_{i,i+1} \in R_{i,i+1}$ route for each unit of medical waste,
$d_i$	Medical waste at $i$ th center,
$dis(x_i, x_{i+1}, r_{i,i+1})$	Distance (km) between $i$ th and $(i+1)$ th centers using $r_{i,i+1} \in R_{i,i+1}$ ,
$c(x_i, x_{i+1}, r_{i,i+1})$	Traveling cost from $i$ th center to $(i+1)$ th center using $r_{i,i+1} \in R_{i,i+1}$ route per unit distance,
$\theta_i$	Occupational risk per unit time for each unit of storage associated with medical waste storage at medical center $i$ ,
$D$	Total collected medical waste,
$L$	Per unit loading cost (INR 30/kg),
$f(x_i, x_{i+1}, r_{i,i+1})$	Fixed charge cost (toll tax) between $i$ th and $(i+1)$ th nodes using $r_{i,i+1} \in R_{i,i+1}$ route,
$f$	Fixed charge cost due to toll tax,
$t(x_i, x_{i+1}, r_{i,i+1})$	Travel time between $i$ th and $(i+1)$ th centers using $r_{i,i+1} \in R_{i,i+1}$ route,
$\tau$	Per unit loading time (2 min/kg),
$w_1, w_2, w_3$	Weighted values for multi-objective,
$h$	Waste amount accumulated per unit time (5 kg/h),
$\xi_i$	Time gap between previous day's clearance and commencement of today's operation at $i$ th node,
$S_i$	Total time upto $i$ th node.
Decision variables:	
$x_{ij}$	Binary decision variable, $x_{ij} = 1$ if the travel from $i$ th node to $j$ th node, else, $x_{ij} = 0$ ,
$\delta(x_i, x_{i+1}, r_{i,i+1})$	Binary decision variable = 1 if medical center is visited $i$ th to $(i+1)$ th using $r_{i,i+1} \in R_{i,i+1}$ route, otherwise 0.

### 3.2. Assumptions/Constraints

- (i) Total collected hazardous COVID-19 medical waste is less than or equal to the capacity of the vehicle.
- (ii) COVID-19 medical waste collectors visit a rural medical center only once and collect the available amount from the center.
- (iii) The COVID-19 medical waste collector starts from a depot/dumping campus with a vehicle and comes back to the same depot/dumping campus after collection.
- (iv) Medical waste collectors have prior ideas/information about the amount of waste at different centers as well as clearance time on the previous day of each center.
- (v) Only one vehicle is considered for collection of COVID-19 medical waste.
- (vi) There are several connecting paths (three in this investigation) between the centers and among the centers and depot/dumping campus.
- (vii) Two input parameters (road congestion and road surface) and one output parameter (accident probability) Type-1 and Type-2 fuzzy logic are considered.
- (viii) The crisp values of input parameters are taken from past records.
- (ix) Type-1 and Type-2 fuzzy logic with 25 rule is used through Type-2 fuzzy logic tool box (Castro et al., 2007).
- (x) Two types of risks (transportation and occupational) due to COVID-19 medical waste are considered.
- (xi) Occupational and transportation risks are determined using number of worker, waste volume, storage duration, accident probability, road conditions, and population density. Most of these parameters are derived from historical data, while accident probability is determined using Type-2 fuzzy logic.

### 3.3. Classical TSP (2DTSP)

Let  $c(i, j)$  be the traveling cost from  $i$ th city to  $j$ th city. Then, classical TSP (CTSP) can be mathematically represented as in Eq. (1).

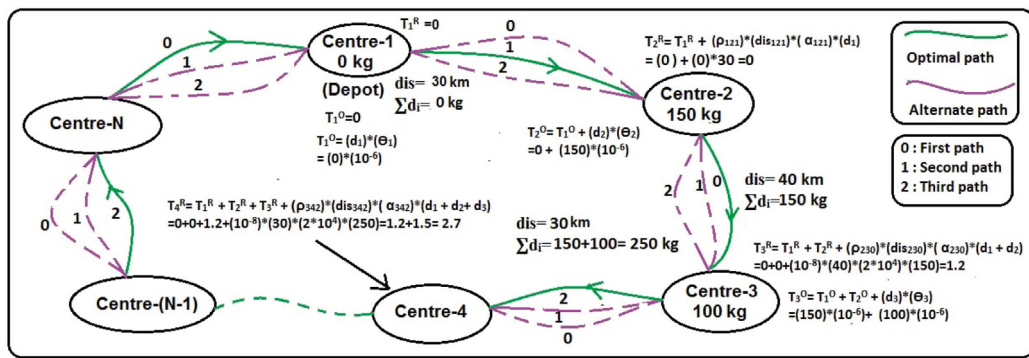
$$\text{minimize } Z = \sum_{i \neq j} c(i, j)x_{ij} \quad (1)$$

$$\begin{aligned} \text{subject to } & \sum_{i=1}^N x_{ij} = 1, \quad j = 1, 2, \dots, N, \\ & \sum_{j=1}^N x_{ij} = 1, \quad i = 1, 2, \dots, N, \\ & \sum_{i \in S} \sum_{j \in S} x_{ij} \leq |S| - 1, \forall S \subset Q, \\ & x_{ij} \in \{0, 1\}, \quad i, j = 1, 2, \dots, N, \quad r \in R_{i,i+1}. \end{aligned} \quad (2)$$

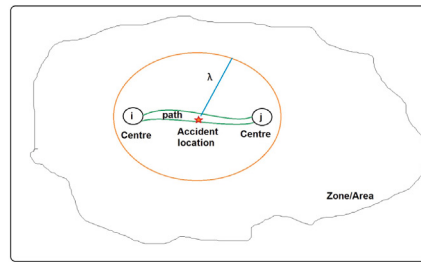
where  $Q = \{1, 2, 3, \dots, N\}$  represents a set of nodes,  $x_{ij}$  are the decision variables. If the salesman travels from  $i$ th city to  $j$ th city, then  $x_{ij} = 1$ , else  $x_{ij} = 0$ . The first two constraints in Eq. (2) imply the visit of a node only once, and the third constraint eliminates the subroute. Then to determine a complete tour  $(x_1, x_2, \dots, x_N, x_1)$  the mentioned CTSP can be represented in Eq. (3). and Eq. (4) satisfied the visit of a node exactly once, and sub tour elimination.

$$\text{minimize } Z = \sum_{i=1}^{N-1} c(x_i, x_{i+1}) + c(x_N, x_1) \quad (3)$$

$$\begin{aligned} \text{subject to } & \sum_{i=1}^N x_{ij} = 1, \quad j = 1, 2, \dots, N, \\ & \sum_{j=1}^N x_{ij} = 1, \quad i = 1, 2, \dots, N, \\ & \sum_{i \in S} \sum_{j \in S} x_{ij} \leq |S| - 1, \forall S \subset Q, \\ & x_{ij} \in \{0, 1\}, \quad i, j = 1, 2, \dots, N. \end{aligned} \quad (4)$$



(a) Graphical representation of model



(b) Transportation risk measurement

Fig. 2. Model illustration and risk measurement.

### 3.4. Multi-path TSP (MPTSP)

Here, we consider the availability of several paths connecting the cities. Let  $c(x_i, x_{i+1}, r_{i,i+1})$  is the traveling cost from  $i$ th city to  $(i+1)$ th city using out of the  $(r_{i,i+1})$ th route per unit distance, where  $r_{i,i+1} \in R_{i,i+1}$ ,  $x_i \in \{1, 2, \dots, N\}$  for  $i = 1, 2, \dots, N$ . Then the problem is in Eq. (5).

$$\text{minimize } Z = \sum_{i=1}^{N-1} c(x_i, x_{i+1}, r_{i,i+1}) \text{dis}(x_i, x_{i+1}, r_{i,i+1}) + c(x_N, x_1, r_{N,1}) \text{dis}(x_N, x_1, r_{N,1}) \quad (5)$$

$$\begin{aligned} \text{subject to } & \sum_{j=1}^N x_{ijr} = 1, \quad j = 1, 2, \dots, N, \\ & \sum_{j=1}^N x_{ijr} = 1, \quad i = 1, 2, \dots, N, \\ & \sum_{i \in S} \sum_{j \in S} x_{ijr} \leq |S| - 1, \forall S \subset Q, \\ & x_{ijr} \in \{0, 1\}, \quad i, j = 1, 2, \dots, N, \quad r_{i,i+1} \in R_{i,i+1}. \end{aligned} \quad (6)$$

Eq. (6) implies that each node is visited only once, also satisfying the subtour elimination constraints.

### 3.5. Medical waste collection problem

A specially equipped medical vehicle with properly dressed collectors moves from a waste disposal center, collects the hazardous waste from different rural health centers/hospitals, and comes back to the dumping campus.

For clarity, the proposed model is illustrated in Fig. 2(a). Here, the starting depot is represented by Center-1 and there is nothing to collect so transportation risk ( $T_1^R$ ) and occupational risk ( $T_1^O$ ) both are zero. Starting from the depot, the vehicle is moved to Center-2 through the

1st path (among the three alternate paths). Now transportation risk is evaluated through Eq. (7) and the value is 0, while occupational risk at Center-2 is evaluated through Eq. (8), and the value is  $(150)(10^{-6})$ . Following this procedure, return to the depot. A detailed step-wise calculation is shown in Fig. 2(a).

In this investigation, three objectives are (cf. Fig. 3) as follows:

- Transportation risk = Accident probability (using Type-2 fuzzy logic) ( $\rho$ ) per unit length  $\times$  length of the road ( $dis$ )  $\times$  indicates the consequence ( $\alpha$ ) of hazardous waste exposure to people and the environment for an accident happening on route (Fig. 2(b) and cf. Taslimi et al. (2017)) for each unit of medical waste  $\times$  cumulative weight of wastage ( $d$ ).
- Occupational risk = Medical waste produced at the center varies with time duration ( $d$ )  $\times$  occupational risk for each unit of storage associated with medical waste storage at the medical center ( $\theta$ ).
- Total cost = Traveling cost ( $c \times dis$ ) + loading cost ( $d \times L$ ) + fixed charge cost due to toll tax ( $f$ ).

### 3.6. Type-1 and Type-2 Fuzzy logic based accident probability

The probability of vehicle accidents on the road is evaluated using Mamdani Type-2 fuzzy logic based on road surface conditions and congestion nature. Here, 25 rules are used (cf. Table 3) where road surface and congestion are input parameters within  $[0, 1]$  and accident probability is the output parameter within  $[10^{-8}, 10^{-5}]$ . Details of Type-1 and Type-2 fuzzy logic are given in Appendix B.

### 3.7. Models of MOMPC-19MWC

We consider the first three models: minimization of transportation risk (Model A, Eqs. (8), (7)), occupational risk (Model B, Eq. (12)), and

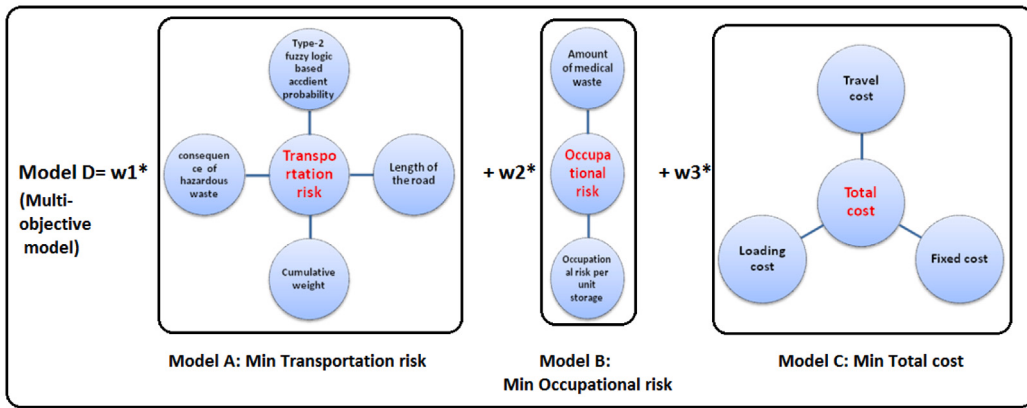


Fig. 3. Four models at a glance.

**Table 3**  
Fuzzy 25 rules.

Road surface	Road congestion	Accident probability
Very smooth	Very rare	Very very low
Very smooth	Rare	Very low
Very smooth	Medium	Very low
Very smooth	Often	Low
Very smooth	Very often	Low
Smooth	Very rare	Very low
Smooth	Rare	Very low
Smooth	Medium	Low
Smooth	Often	Low
Smooth	Very often	Medium
Medium	Very rare	low
Medium	Rare	low
Medium	Medium	Medium
Medium	Often	Medium
Medium	Very often	High
Rough	Very rare	Medium
Rough	Rare	Medium
Rough	Medium	High
Rough	Often	High
Rough	Very often	Very high
Very rough	Very rare	High
Very rough	Rare	High
Very rough	Medium	Very high
Very rough	Often	Very high
Very rough	Very often	Very very high

total cost (Model C, Eqs. (9), (13)). These three models are individual, single-objective problems. The last model (Model D) is the multi-objective model using the weighted sum method (minimization of the above three objectives).

### 3.7.1. Model A: Minimization of transportation risk

The model is mathematically formulated as:

$$\begin{aligned}
 & \text{minimize } T^R = \\
 & \sum_{i=1}^{N-1} \underbrace{[\rho(x_i, x_{i+1}, r_{i,i+1}) dis(x_i, x_{i+1}, r_{i,i+1}) \alpha(x_i, x_{i+1}, r_{i,i+1})]}_{\substack{\text{Accident Probability} \\ i}} \underbrace{dis(x_i, x_{i+1}, r_{i,i+1})}_{\text{Distance}} \underbrace{\alpha(x_i, x_{i+1}, r_{i,i+1})}_{\text{Consequence}} \\
 & \times \sum_{j=1}^N d_j \underbrace{\delta(x_i, x_{i+1}, r_{i,i+1})}_{\substack{\text{Waste} \\ \text{Binary Variable}}} \\
 & + [\rho(x_N, x_1, r_{N,1}) dis(x_N, x_1, r_{N,1}) \alpha(x_N, x_1, r_{N,1}) \sum_{j=1}^N d_j] \\
 & \times \underbrace{\delta(x_N, x_1, r_{N,1})}_{\substack{\text{Binary Variable}}}
 \end{aligned} \quad (7)$$

$$O^R = \sum_{i=2}^N (d_i \theta_i), \quad (8)$$

$d_i = \underbrace{S_i h}_{\substack{\text{Storage} \times \text{per unit} \\ \text{Occupational risk}}}, \quad \underbrace{Time \times \text{per unit amount}}$

$$\begin{aligned}
 Z = & \underbrace{\sum_{i=1}^{N-1} c(x_i, x_{i+1}, r_{i,i+1}) dis(x_i, x_{i+1}, r_{i,i+1}) + c(x_N, x_1, r_{N,1}) dis(x_N, x_1, r_{N,1})}_{\substack{\text{Traveling Cost}}} \\
 & + \underbrace{\sum_{i=2}^N (d_i L)}_{\substack{\text{Loading Cost}}} + \underbrace{\sum_{i=1}^{N-1} f(x_i, x_{i+1}, r_{i,i+1}) \delta(x_i, x_{i+1}, r_{i,i+1}) + f(x_N, x_1, r_{N,1}) \delta(x_N, x_1, r_{N,1})}_{\substack{\text{Fixed Charge Cost}}}
 \end{aligned} \quad (9)$$

$$\begin{aligned}
 S_k = & \underbrace{\sum_{i=1}^{k-1} t(x_i, x_{i+1}, r_{i,i+1}) dis(x_i, x_{i+1}, r_{i,i+1}) + t(x_k, x_1, r_{k,1}) dis(x_k, x_1, r_{k,1})}_{\substack{\text{Traveling Time}}} \\
 & + \underbrace{\sum_{i=2}^k (d_i \tau)}_{\substack{\text{Loading Time}}} + \underbrace{\xi_i}_{\text{Time Gap}}
 \end{aligned} \quad (10)$$

$$\sum_{i=1}^N d_i = D, \quad d_1 = 0, \quad r_{i,i+1} \in R_{i,i+1}. \quad (11)$$

Here, minimization of the transportation risk (Eq. (7)),  $\rho(x_i, x_{i+1}, r_{i,i+1})$  represents accident probability per unit length from  $i$ th node to  $(i+1)$ th node using  $r_{i,i+1} \in R_{i,i+1}$  route, which is evaluated through Type-2 fuzzy logic based on road surface and congestion. The distance from  $i$ th center to  $(i+1)$ th center using  $r_{i,i+1} \in R_{i,i+1}$  route is through  $dis(x_i, x_{i+1}, r_{i,i+1})$ . Again,  $\alpha(x_i, x_{i+1}, r_{i,i+1})$  indicates the consequence of hazardous waste exposure to people and the environment for an accident happening from  $i$ th center to  $(i+1)$ th center using  $r_{i,i+1} \in R_{i,i+1}$  route for each unit of medical waste. Also,  $\sum_{i=1}^N d_i$  indicates the carried cumulative medical waste and  $\delta(x_i, x_{i+1}, r_{i,i+1})$  is a binary decision variable = 1 if medical center is visited  $i$ th to  $(i+1)$ th using  $r_{i,i+1} \in R_{i,i+1}$  route, otherwise 0.

Eq. (8) is used to determine the value of occupational risk, where  $\theta_i$  is the occupational risk for each unit of storage associated with medical waste storage at medical center  $i$ . Again,  $d_i = S_i \times h$  indicates the medical waste that increases concerning time, where  $S_i$  is the total time

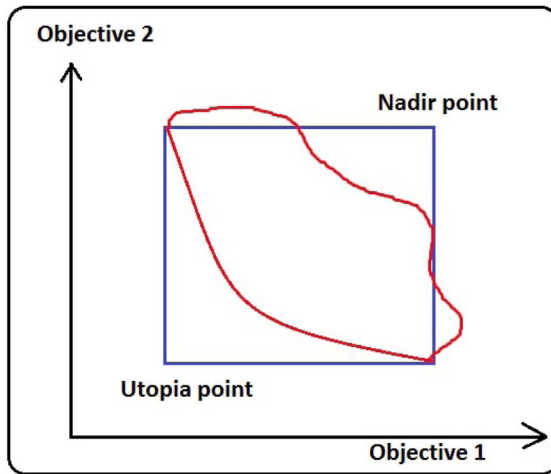


Fig. 4. Adaptive weighted method.

up to  $i$ th node and  $h$  is the waste amount accumulated per unit time.

In Eq. (9), objective function  $Z$  is the total cost, and it has three parts: the first indicates the traveling cost ( $c \times dis$ ), the second the loading cost ( $d \times L$ ) of the medical waste, and the third for a fixed charge ( $f$ ), due to toll tax through out the routing. Here, the occupational risk and total cost are calculated for minimum transportation risk. Eq. (10) indicates the total time up to  $k$ th node, including previous traveling time, loading time, and  $\xi_i$  (time gap between the previous day's clearance and commencement of today's operation). Eq. (11) consists of three parts. The first part states that the total collected medical waste equals the collected COVID-19 medical waste from individual medical centers. The second part indicates that there is no medical waste to collect at the depot/dumping center. The third part illustrates the available multi-path between two arbitrary medical centers.

### 3.7.2. Model B: Minimization of occupational risk

$$\text{minimize } O^R, \quad (12)$$

along with the corresponding  $T^R$ ,  $Z$  and  $S_k$  (Eqs. (7), (9), (10)), where  $O^R$  is given by Eq. (8)

### 3.7.3. Model C: Minimization of total cost

$$\text{minimize } Z, \quad (13)$$

along with the corresponding  $T^R$ ,  $O^R$  and  $S_k$  (Eqs. (7), (8), (10)), where  $Z$  is given in Eq. (9).

### 3.7.4. Model D: Multi-objective model (minimization of transportation risk, occupational risk, and total cost)

A weighted sum of normalized values of the three objective functions is used (Kim and De Weck, 2006).

The model is mathematically formulated as:

$$\begin{aligned} \text{minimize } B &= w_1(T^R - T_{Utopia}^R)/T_{Nadir}^R + w_2(O^R - O_{Utopia}^R)/O_{Nadir}^R \\ &\quad + w_3(Z - Z_{Utopia})/Z_{Nadir}, \end{aligned} \quad (14)$$

subject to  $w_1 + w_2 + w_3 = 1$ .

Utopia and Nadir points are depicted in Fig. 4. Eq. (14) introduces a multi-objective model derived using the normalization concept. It comprises three parts: the first, second, and third parts represent normalization based on transportation risk, occupational risk, and total system cost of the model, respectively. These operations are conducted

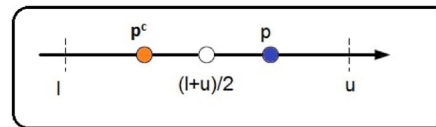


Fig. 5. Example of opposition base point.

with reference to the Nadir points and Utopia points of the single objective problems.

## 4. Proposed partial opposition-based genetic algorithm

As the above models are NP-hard in nature. To solve those real-life problems, we used a heuristic algorithm named the Proposed partial opposition-based genetic algorithm (POBGA). We consider the first three models: minimization of transportation risk (Model A), occupational risk (Model B), and total cost (Model C). These three models are individual, single-objective NP-hard problems. The last model (Model D) is the multi-objective model using the weighted sum method (minimization of the above three objectives). To handle these real-life problems, we incorporated partial opposition-based initialization and mutation in the proposed genetic algorithm. Also, we design problem-specific crossover (weighted crossover) to get near-optimal solutions in an efficient manner.

### 4.1. Representation

Let there be  $M$  paths covering  $N$  cities. For  $i$ th path,  $N$ -dimensional integer vectors  $X_i = (x_{i1}, x_{i2}, \dots, x_{iN})$  are created where  $x_{i1}, x_{i2}, \dots, x_{iN}$  indicate  $N$  consecutive nodes in a tour. Here,  $x_{ij}$ ,  $i = 1, 2, \dots, M$  and  $j = 1, 2, \dots, N$  are randomly generated by a random number generator function between 1 to  $N$  maintaining the TSP conditions. As the population size is  $M$ ,  $M$  numbers of chromosomes are randomly generated.

### 4.2. Opposition-based learning

Mainly opposition-based learning is used for solving continuous optimization problems. Opposition-based learning is basically implemented to create diversity in continuous search space. Focusing on that, we want to solve combinatorial/discrete optimization problems.

The opposition-based concept in the continuous domain, for  $D$  dimensional vectors ( $R^D$ ), is first introduced by (cf. Tizhoosh, 2005). Assume,  $L = (p_1, p_2, \dots, p_D)$  be any point in  $R^D$ , where  $p_1, p_2, \dots, p_D \in R$  and  $p_i \in [l_i, u_i]$ ,  $\forall i \in 1, 2, \dots, D$ . The opposite point  $L^c = (p_1^c, p_2^c, \dots, p_D^c)$  defined as  $p_i^c = l_i + u_i - p_i$ . Here, the opposite point of  $p$  (in one dimensional) is shown in Fig. 5.

#### 4.2.1. Partial opposition-based learning (POBL)

Hu et al. (2014) proposed POBL, a better form of OBL the scheme, in the literature on Adaptive Differential Evolution (ADE) algorithm. Si and Dutta (2019) applied POBL in PSO for Artificial Neural Network training for medical data classification, and POBL improved the exploration ability of PSO resulting in better performance. In a multi-dimensional search space, an opposite point contains opposite values of original values in each dimension in OBL. In a multi-dimensional space, the partial opposite point contains opposite numbers to the original numbers in some dimensions. Till the POBL is used only on continuous optimization. The concept of POBL is applied to this investigation. From a single solution (chromosome), generate two other opposite solutions.

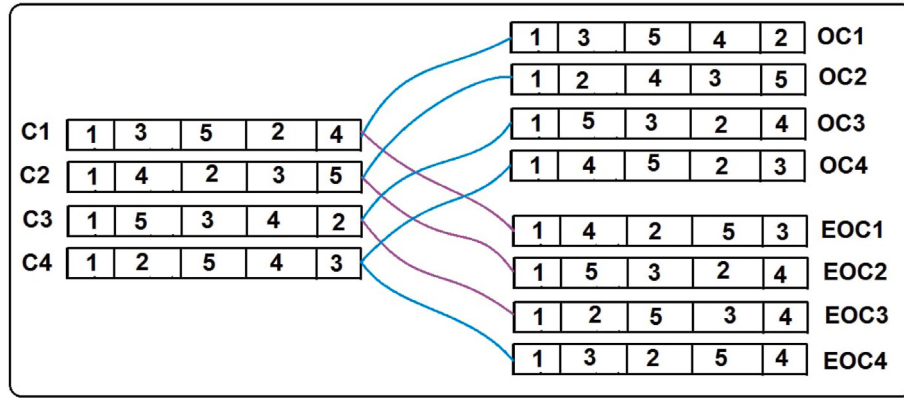


Fig. 6. Opposition base initialization.

#### 4.3. Initialization

Using the POBL approach in initialization is shown in Fig. 6 of the proposed algorithm, let us consider that the first node is fixed (depot), represented by 1 and initial population size = 4. Then, after using partial opposition-based learning, the population size becomes  $4 + 4 + 4 = 12$ . Now, we select the best 4 out of 12 chromosomes using Section 4.4.

#### 4.4. Selection (Probabilistic selection)

We first calculate the Boltzmann-Probability (Maity et al., 2015) for each chromosome of the initial population using Eq. (15).

$$p_B = e^{((g/G)(f_{min} - f(X_i))/KT)}, \quad (15)$$

Here,  $T = T_0(1 - a)^k$ ,  $k = (1 + C \times \text{rand}[0, 1])$ ,  $C = \text{rand}[1, 100]$ ,  $g$  = current generation number,  $G$  = max-gen,  $T_0 = \text{rand}[50, 140]$ ,  $a = \text{rand}[0, 1]$ ,  $f(X_i)$  is the objective function,  $f_{min} = \min f(X_i)$ ,  $i = 1, 2, \dots, N$ .

For the mating pool, the following process is followed: First, a predefined value, say the probability of selection ( $p_s$ ) is assigned. If each chromosome of  $f(X_i)$ , a random number,  $r \in [0, 1]$  is generated. If  $r < p_s$  or  $r < p_B$ , then the corresponding chromosome is selected for the mating pool. Otherwise, chromosomes corresponding to  $f_{min}$  are selected for the mating pool. Finally, out of these chromosomes, 4 chromosomes are selected for crossover.

#### 4.5. Crossover (Weighted crossover)

Initially, two individuals (parents) are selected randomly from the mating pool based on the random number generated between  $[0, 1]$ . Select the first parent (say  $P_1$ ) according to  $r < p_c$ . Similarly, another parent (say  $P_2$ ) is selected. Out of these parents, children are created using the weighted crossover. First, evaluate the weighted value, using Eq. (16), of each path between the centers; then, based on the minimum weighted value, the crossover is performed.

$$w(x_i, x_{i+1}, r) = \frac{1}{4} [\alpha \frac{c(x_i, x_{i+1}, r_{i,i+1}) dis(x_i, x_{i+1}, r_{i,i+1})}{\sum_{j=1}^{N-1} c(x_i, x_{i+1}, r_{i,j+1}) dis(x_i, x_{i+1}, r_{i,j+1}) + c(x_N, x_1, r_{N,1}) dis(x_N, x_1, r_{N,1})} \\ + \beta \frac{(d_i L)}{\sum_{i=2}^N (d_i L)} + \gamma \frac{f(x_i, x_{i+1}, r_{i,i+1}) \delta(x_i, x_{i+1}, r_{i,i+1})}{\sum_{i=1}^{N-1} f(x_i, x_{i+1}, r_{i,i+1}) \delta(x_i, x_{i+1}, r_{i,i+1}) + f(x_N, x_1, r_{N,1}) \delta(x_N, x_1, r_{N,1})} \\ + \delta_1 \frac{\rho(x_i, x_{i+1}, r_{i,i+1}) \sum_{j=1}^i d_j dis(x_i, x_{i+1}, r_{i,j+1}) \delta(x_i, x_{i+1}, r_{i,j+1})}{T^R} + \delta_2 \frac{(d_i \eta_i(d_i \tau))}{O^R}]. \quad (16)$$

Eq. (16) comprises five components. The initial three components pertain to the cost aspects of the model, specifically the normalized

travel cost, loading cost, and fixed charge cost. The fourth and fifth components involve the normalization of transportation and occupational risks, respectively. This represents a problem-specific, weighted crossover approach. Here, consider  $\alpha = \beta = \gamma = 0.11$  and  $\delta_1 = \delta_2 = 0.335$ . The procedure to produce offspring is illustrated with an example for five node TSP (Fig. 7).

As we use comparison crossover and starting node of two parents are the same (1) so, to generate a second child, we update (reverse) the nodes of the second parent as shown in Fig. 7(d). After that, follow the same process for the second child as the first one.

#### 4.6. Mutation

##### 4.6.1. Generation-dependent partial opposition-based learning (POBL) mutation

Here, we formulate a novel generation-dependent OB mutation. Here generation-based probability of mutation ( $p_m$ ) is evaluated as  $p_m = \frac{t}{g}$ ,  $t \in (0, 1)$ .  $g$  represents the current generation number.

##### 4.6.2. Mutation process

If  $r < p_m$ ,  $r \in \text{rand}[0, 1]$ , then the corresponding chromosome is selected for mutation. Partial opposition-based mutation (except for 1st and the last node, as the depot is fixed) shown in Algorithm 1 and in Fig. 8.

---

**Algorithm 1:** GENERATION-DEPENDENT POBL MUTATION

---

**Input:** Selected chromosome  
**Output:** Mutated chromosome  
1 Set  $g = \text{current generation number}$   
2  $p_m = \frac{t}{g}$ ,  $t \in (0, 1)$   
3 **for**  $i \leftarrow 0$  **to**  $pop\_size$  **do**  
4      $r = \text{rand}(0, 1)$   
5     **if** ( $r < p_m$ ) **then**  
6         Choose current solution  $a_i$ , ( $i=1, \dots, N$ )  
7         Mutated solution  $m_i = (1+N) - a_i$  and  
8          $m'_i = a_{N-i}$  ( $i=2, \dots, N-1$ ) (cf. Fig. 8)

---

After the selection, crossover and mutation procedures are obtained. If  $\text{rand}(0, 1)$  is less than the opposition jumping rate ( $J R$ ), then the total population is the existing population (4) and created opposition-based population (4 + 4) and, from these 12 chromosomes, we select the best 4 chromosomes as per Section 4.4.

A combination of the above steps leads to the proposed POBGA presented in Algorithm 2 and flowchart given in Fig. 9.

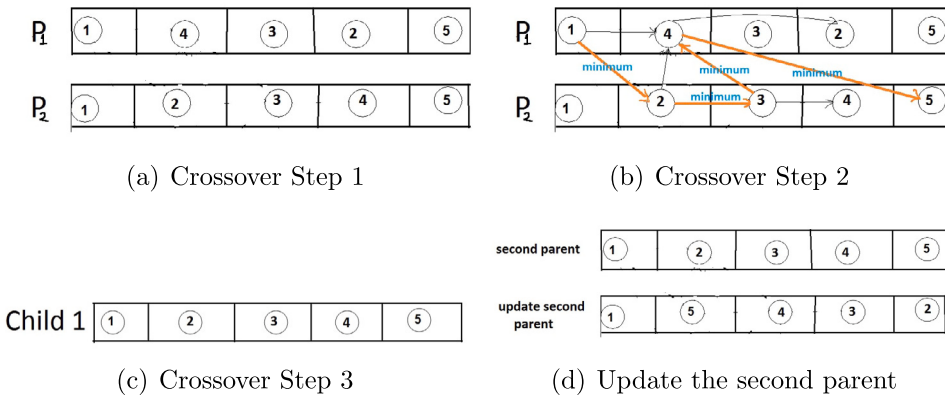


Fig. 7. Comparison crossover for child 1 and 2.

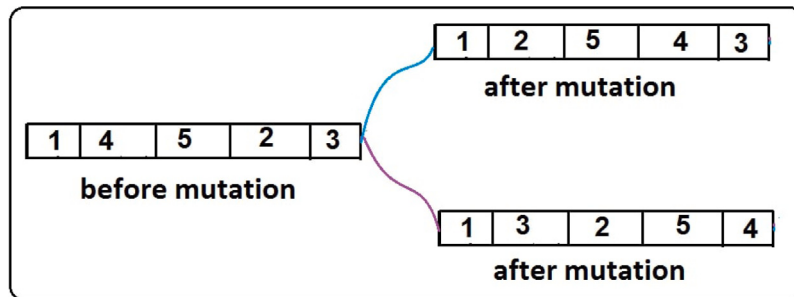


Fig. 8. Mutation process.

**Algorithm 2:** PARTIAL OPPONENT-BASED GENETIC ALGORITHM (POBGA)

**Input:** pop size, jumping rate ( $JR$ ), current generation ( $g$ ), and maximum generation ( $G$ )  
**Output:** Set of optimum solutions

- 1 Start
- 2 Randomly generate initial population ( $M$ )
- 3 POBL population generated using Section 4.2 ( $M' + M''$ )
- 4  $g=1$
- 5 **while** ( $g \leq G$ ) **do**
- 6     Selecting  $M$  fittest solutions from ( $M + M' + M''$ ) using Section 4.4
- 7     Weighted crossover using Section 4.5
- 8     Generation dependent POBL mutation according to Algorithm 1
- 9     **if** ( $\text{rand}(0, 1) < JR$ ) **then**
- 10         Evaluate the opposite population ( $M' + M''$ ) of the current population ( $M$ )
- 11      $g \leftarrow g + 1$
- 12 Store the global optimum and near optimum values

**5. Validation of the developed POBGA**

The developed POBGA is tested against some test functions from TSPLIB (Reinelt, 1995), and its supremacy is established through a statistical test. These are presented in Appendix C.

**6. Numerical experiments: A real-life illustration**

We consider the case of COVID-19 medical waste collection in the BANKURA district, West Bengal, India (cf. 15). There is a main

hospital cum medical waste dumping center, Bankura Sammilani Medical College (marked by '1'), and 9 medical waste collection centers ((2) Barjara, (3) Health World, (4) HLC Memorial, (5) Dubrajpur, (6) Ramsagar, (7) Sanaka Hospital, (8) Gangajalghati, (9) Puncha, and (10) Mission). The distance, traveling cost per unit distance, fixed charge cost, and time matrices (row-wise from Google Map, 2nd, 3rd, and from Google Map sets correspond to distances, traveling cost per unit distance, fixed charge cost, and time) for MOMPC-19MWCP are presented in Table [https://github.com/somnathmajivucs/COVID-19\\_medical\\_waste\\_collection\\_problem/blob/main/input\\_table](https://github.com/somnathmajivucs/COVID-19_medical_waste_collection_problem/blob/main/input_table). As mentioned earlier, there are three types of routes between every two centers with the corresponding distances, traveling costs, and traveling times matrices. For the distance, traveling cost, and traveling time (a,b,c), where the values a, b, and c are for the 1st, 2nd, and 3rd routes, respectively.

**6.1. Input data**

For the experiment, we consider MOMPC-19MWCP with 10 nodes (places) and 3 alternative paths between every two nodes. The distance, traveling cost per unit distance, fixed charge cost, and time matrices (Row-wise 1st, 2nd, 3rd, and 4th sets correspond to distances, traveling cost per unit distance, fixed charge cost, and time) for MOMPC-19MWCP are presented in Table [https://github.com/somnathmajivucs/COVID-19\\_medical\\_waste\\_collection\\_problem/blob/main/input\\_table](https://github.com/somnathmajivucs/COVID-19_medical_waste_collection_problem/blob/main/input_table).

The proposed algorithm POBGA is the combination of probabilistic selection, weighted crossover, and generation-dependent POBL mutation, which was implemented in C++ with 150 chromosomes and 1000 iterations at maximum. It is implemented using the Codeblock compiler on a 5th Gen. Intel Core i5 CPU @ 3 GHz. The proposed MOMPC-19MWCP is solved and numerically illustrated by the newly implemented POBGA for some input data.

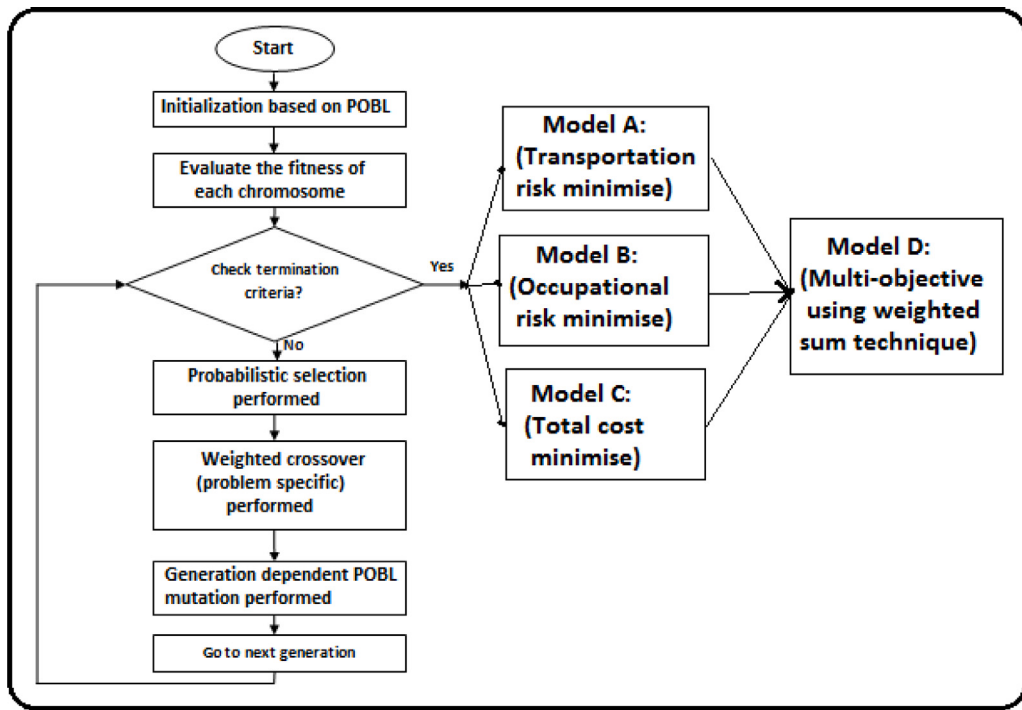


Fig. 9. Flow chart of proposed method and model.

**Table 4**  
Clearance time on previous day.

Nodes	1	2	3	4	5	6	7	8	9	10
Previous day clearance times	0	10 AM	3 PM	4 PM	11 AM	1 PM	10:30 AM	3 PM	2 PM	2:30 PM

**Table 5**  
Parameters values chosen for numerical experiment.

Parameters	Value/Range	Parameters	Value/Range
Max_Generation	200–1000	$h$	5 kg/h
Number of Chromosome	50–150	$p_m$	0.31
$p_c$	0.49	$\tau$	2 min/kg
$JR$	0.34	Road congestion	(0,1)
$L$	INR 30	Population density	2664/square mile
Road surface	(0,1)	$\alpha$	$10^5$
Accident probability	$(10^{-5}–10^{-8})$		
Occupational risk ( $\theta$ )	$10^{-6}$		

As mentioned earlier, there are three types of routes between two nodes with the corresponding distance and traveling cost matrices along different routes for the models. For the distance and traveling cost  $(a, b, c)$  (represented by  $(\equiv (0, 1, 2))$ ) (say), the values  $a$ ,  $b$ , and  $c$  are for the 1st, 2nd and 3rd routes respectively. Clearance time on the previous day's matrix of nodes is given in Table 4. West Bengal has a population density of 2664 people per square mile at present. The values of the parameter are given in Table 5.

## 6.2. Routing problems (Models-A and B) having single path between the nodes

Instead of multi-paths, we assume that there is only one route for travel between the nodes. Taking a particular path ('0' in this case); the routing problem is solved and results are given in Tables 6, 7, 8, and 9.

## 6.3. Optimum results of MOMPC-19MWCP

Here, we present the optimum results of the models with multi-paths and single path (taking '0'-th path) taking three (Table 10) and two objectives (Tables 11, 12, 13 for multi-path only) at a time. Total cost is also evaluated and graphically presented with two risks as constraints (Table 9 and Figs. 10(a) and 10(b)). Model D is further optimized by assigning different weights to the objectives, and optimum results are graphically presented in Fig. 11. The Pareto fronts for the optimal results in Tables 11, 12, 13 are depicted in Figs. 12(a)–12(f) respectively.

### 6.3.1. Optimum transportation risk (Model A)

The results of the optimum transportation risk are presented in Table 6.

**Table 6**  
Optimum transportation risk.

Parameters	With multi-path	With single path
Path	1(1)-6(0)-4(0)-5(0) -9(2)-10(0)-2(0)-3(0) -7(2)-8(0)-1	1(0)-6(0)-10(0)-2(0) -5(0)-9(0)-4(0)-3(0) -7(0)-8(0)-1
Distance (km)	213	228
Traveling cost (INR)	1869	2006
Loading cost (INR)	4110	4110
Fixed charge (INR)	199	90
Total cost (INR)	6178	6206
Transportation risk	34.17	44.41
Occupational risk	$3.93 \times 10^{-4}$	$4.07 \times 10^{-4}$
Travel time (min)	317	341
Loading time (min)	152	152
Total time (min)	469	493

**Table 7**  
Optimum occupational risk.

Parameters	With multi-path	With single path
Path	1(1)-6(0)-4(0)-5(0) -8(2)-7(0)-10(2)-2(2) -3(2)-4(2)-1	1(0)-6(0)-5(0)-7(0) -8(0)-9(0)-10(0)-2(0) -3(0)-4(0)-1
Distance (km)	237	231
Traveling cost (INR)	2139	2257
Loading cost (INR)	4110	4110
Fixed charge (INR)	194	181
Total cost (INR)	6443	6548
Transportation risk	57.32	48.25
Occupational risk	$3.7 \times 10^{-4}$	$3.9 \times 10^{-4}$
Travel time (min)	342	317
Loading time (min)	152	152
Total time (min)	494	469

**Table 8**  
Optimum total cost.

Parameters	With multi-path	With single path
Path	1(1)-6(0)-4(0)-5(0) -9(1)-8(2)-7(1)-10(0) -2(0)-3(2)-1	1(0)-6(0)-4(0)-9(0) -5(0)-7(0)-8(0)-10(0) -2(0)-3(0)-1
Distance (km)	211	228
Traveling cost (INR)	1838	1932
Loading cost (INR)	4110	4110
Fixed charge (INR)	78	86
Total cost (INR)	6026	6128
Transportation risk	42.99	61.00
Occupational risk	$3.98 \times 10^{-4}$	$4.38 \times 10^{-4}$
Travel time (min)	317	339
Loading time (min)	152	152
Total time (min)	469	491

### 6.3.2. Optimum occupational risk (Model B)

The results of the optimum occupational risk are presented in Table 7.

### 6.3.3. Optimum total cost (Model C)

The results of the optimum total cost are presented in Table 8.

### 6.3.4. Optimum results of model D (Multi-objective)

The results of optimum Transportation risk, Occupational risk, and total cost are presented in Table 10 and Fig. 11.

### 6.3.5. Optimum results of transportation and occupational risk (Multi-objective)

The results of optimum Transportation risk and Occupational risk are presented in Table 11 and Figs. 12(e), 12(f).

### 6.3.6. Optimum results of transportation risk and total cost (Multi-objective)

The results of optimum Transportation risk and total cost are presented in Table 12 and Figs. 12(a), 12(b).

### 6.3.7. Optimum results of occupational risk and total cost (Multi-objective)

The results of optimum Occupational risk and total cost are presented in Table 13 and Figs. 12(c), 12(d).

### 6.3.8. Results compared between Type-1 and Type-2 fuzzy logic

The comparison conducted between Type-1 and Type-2 fuzzy logic-based transportation risk, as depicted in Fig. 13, reveals that the Type-2 fuzzy logic-based system outperforms its Type-1 counterpart based on experimental results.

Once more, all results concerning transportation risk are juxtaposed with both Type-1 and Type-2 fuzzy logic. Notably, it is evident, as seen in Fig. 14, that across all scenarios, Type-2 fuzzy logic consistently outperforms Type-1 fuzzy logic.

Type-2 fuzzy models are renowned for their superior handling of uncertainties compared to Type-1 models, with at the expense of increased computational complexity. This investigation meticulously examines strategies for managing this complexity and quantifies its impact on runtime, as outlined in detail in Table 14. For small-scale problems (involving 10 nodes in this investigation), the impact on runtime complexity is minimal. However, as the problem size grows, particularly with larger nodes, the computational complexity escalates significantly. Parameter tuning is performed in this study (see Tables A.1 and A.2, Figs. A.3 and A.4 in the Appendix), after which we fixed the study to 25 rules in the Type-2 fuzzy logic system.

## 7. Dissection of the optimum results

From Table 6, it is observed that the use of multi-path between the nodes gives less transportation, occupational risks, and total cost than the single path model. The same results are found for other models (Tables 7, 8)

In Table 6, the multi-path with minimized transportation risk is 1(1)-6(0)-4(0)-5(0)-9(2)-10(0)-2(0)-3(0)-7(2)-8(0)-1. The distance, traveling cost, loading cost, fixed charge, total cost, transportation risk, occupational risk, traveling time, loading time, and total time are 213 km, INR 1869, INR 4110, INR 199, INR 6178, 34.17,  $3.93 \times 10^{-4}$ , 317 min, 152 min, and 469 min respectively.

Table 9 represents the total cost with two risks-transportation and occupational as constraints. It is seen that when the transportation risk limit decreases, the total cost increases (Fig. 10(a)), but when the transportation risk limit is less than 36, it is unable to find the feasible path in the system. Again when risk increases, the total cost is minimized up to a certain level (43). When the risk is above 43, the total cost remains unaltered (cf. Table 9). This behavior is as per expectation.

Similar scenarios are observed for occupational risk limit (cf. Table 9). Also for this model, when the risk limit decreases, the total cost increases (Fig. 10(b)), but when the risk limit is less than  $3.65 \times 10^{-4}$ , we do not get any feasible path in the system. Again when risk is increased, the total cost is minimized up to a certain level ( $4.0 \times 10^{-4}$ ) and beyond this level, the total cost remains unaltered.

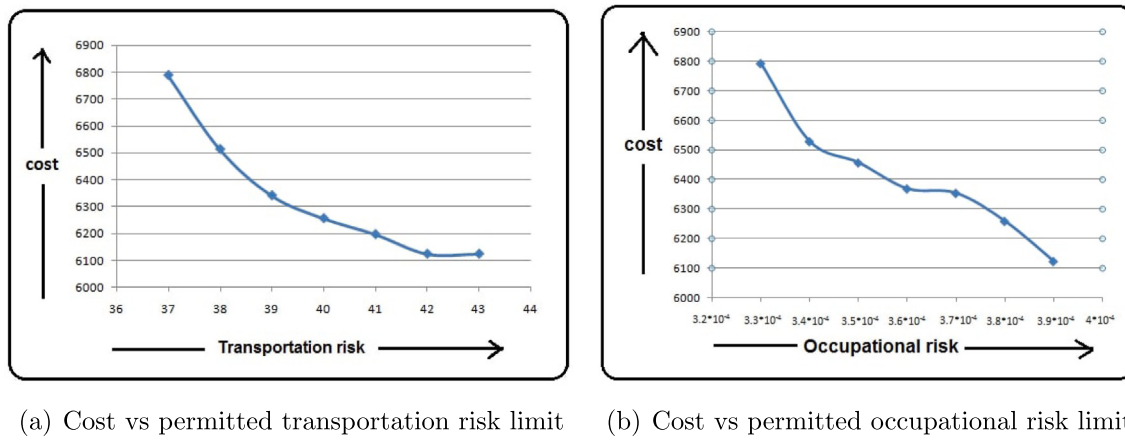
Table 9 also furnishes that multi-path routing gives feasible paths with much lower risks, which is not possible for the single-path routing model.

Through Fig. 11, we can observe the performance of the multi-objective model considering total cost, transportation risk, and occupational risk. It is observed that total cost increases when both risk limits decrease. Figs. 12(a), 12(b) represents how transportation risk and total cost behave using POBGA and GA (Roulette wheel selection, cyclic crossover, and random mutation) for multi-path and single path. It is observed that POBGA with multi-path gives better performance.

**Table 9**  
Optimum total cost with different risk limits as constraint

Transportation risk			Occupational risk		
Risk limit	Total cost (with multi-path)	Total cost (with single path)	Risk limit	Total cost (with multi-path)	Total cost (with single path)
50	6026 (same)	7342 (same)	$4.35 \times 10^{-4}$	6026 (same)	8146 (same)
49	6026 (same)	7342 (same)	$4.30 \times 10^{-4}$	6026 (same)	8146 (same)
48	6026 (same)	7164	$4.25 \times 10^{-4}$	6026 (same)	8146 (same)
47	6026 (same)	6752	$4.20 \times 10^{-4}$	6026 (same)	7891
46	6026 (same)	6418	$4.15 \times 10^{-4}$	6026 (same)	7516
45	6026 (same)	6253	$4.10 \times 10^{-4}$	6026 (same)	7352
44	6026 (same)	NFS	$4.05 \times 10^{-4}$	6026 (same)	7181
43	6026 (same)	NFS	$4.0 \times 10^{-4}$ and above	6026 (same)	6712
42	6125	NFS	$3.95 \times 10^{-4}$	6123	6548
41	6198	NFS	$3.90 \times 10^{-4}$	6259	NFS
40	6257	NFS	$3.85 \times 10^{-4}$	6354	NFS
39	6342	NFS	$3.80 \times 10^{-4}$	6379	NFS
38	6514	NFS	$3.75 \times 10^{-4}$	6457	NFS
37	6789	NFS	$3.70 \times 10^{-4}$	6529	NFS
36	6932	NFS	$3.65 \times 10^{-4}$ and below	NFS	NFS
35	NFS	NFS			

NFS: No feasible solution.



(a) Cost vs permitted transportation risk limit

(b) Cost vs permitted occupational risk limit

Fig. 10. Graphical representation of risk and cost.

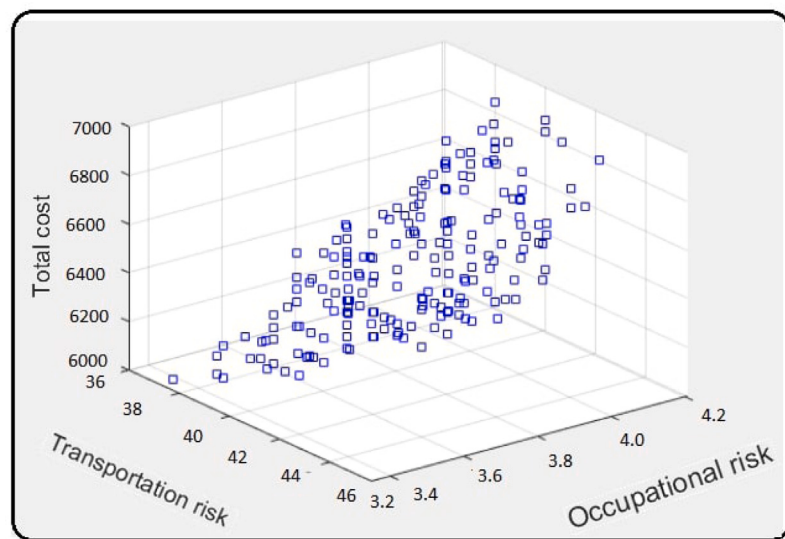


Fig. 11. Results of Model D using different weights.

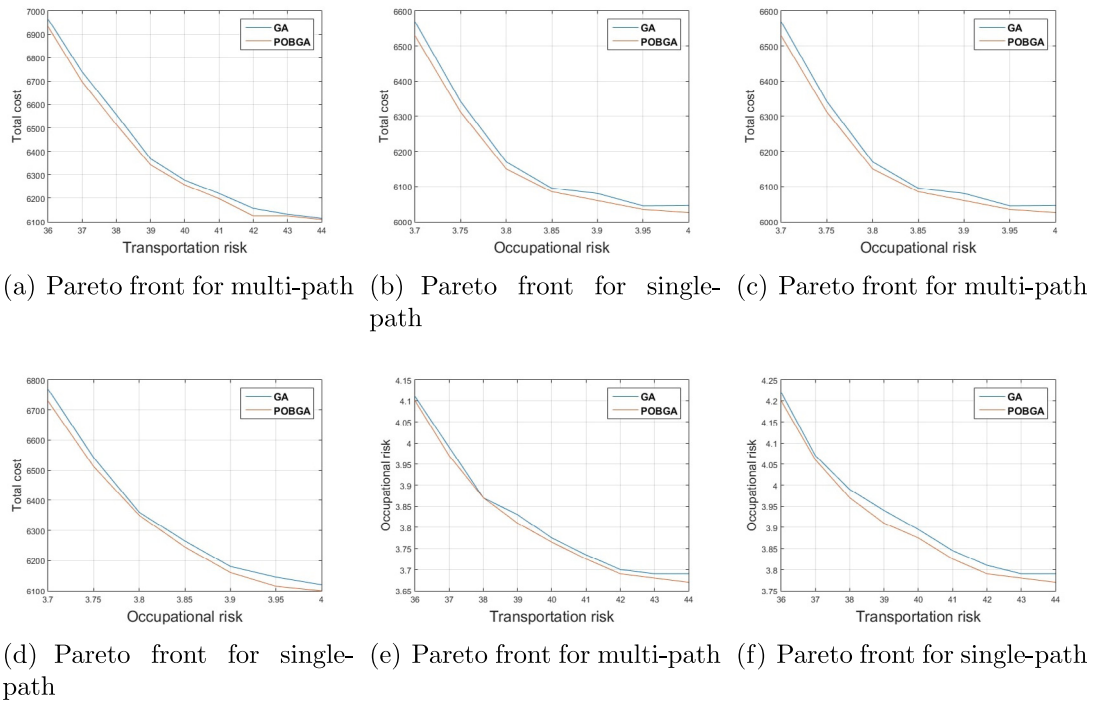


Fig. 12. Representation of risk and cost for single and multi objective.

**Table 10**  
Results of Model D.

$w_1$	$w_2$	$w_3$	$T^R$	$O^R$	Total cost
.33	.33	.34	34.17	$3.93 \times 10^{-4}$	6178
.1	.1	.8	39.10	$3.87 \times 10^{-4}$	6027
.1	.8	.1	37.68	$3.83 \times 10^{-4}$	6109

**Table 11**  
Results of transportation and occupational risk.

$w_1$	$w_2$	$T^R$	$O^R$
.50	.50	44.56	$3.81 \times 10^{-4}$
.1	.9	34.82	$3.96 \times 10^{-4}$
.9	.1	53.16	$3.68 \times 10^{-4}$

**Table 12**  
Results of transportation risk and total cost.

$w_1$	$w_3$	$T^R$	Total cost
.50	.50	45.23	6216
.1	.9	36.19	6438
.9	.1	53.98	6112

**Table 13**  
Results of occupational risk and total cost.

$w_2$	$w_3$	$O^R$	Total cost
.50	.50	$3.82 \times 10^{-4}$	6276
.1	.9	$3.73 \times 10^{-4}$	6398
.9	.1	$3.96 \times 10^{-4}$	6071

Figs. 12(c) and 12(d) represent how occupational risk and total cost behave using POBGA and GA. Figs. 12(e) and 12(f) represent how occupational risk and transportation risk behave using POBGA and GA. In all the cases it is observed that POBGA with multi-path gives better performance.

Through a series of computational experiments conducted meticulously, the consistent trend emerges, revealing that across all scenarios

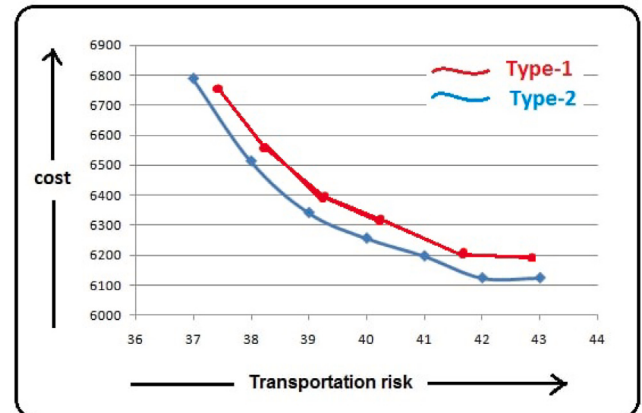


Fig. 13. Transportation risk using Type-1 and -2 fuzzy logic.

and test cases, Type-2 fuzzy logic consistently demonstrates superior performance compared to Type-1 fuzzy logic (cf. Figs. 13, 14).

All the Figs. (cf. Fig. 15) are presented for the route schedules/routing plan obtained by POBGA for different models. It is observed that the routing plans are changed concerning different models. The management can make proper decisions as per their requirement.

### 7.1. Performance metrics

The statistical data corresponding to the performance measures — ONVG, OTNVG, OTNVGR, and ER are shown in Table 15. This table shows that for each of the test examples, the proposed algorithm yields the largest percentage value of OTNVGR. In light of the OTNVGR measure, the proposed algorithm performs better than the other methods that were taken into consideration. These statistics also show that the ER values of the Pareto optimum fronts produced by the suggested algorithm are minimal in every case. Therefore, when compared to

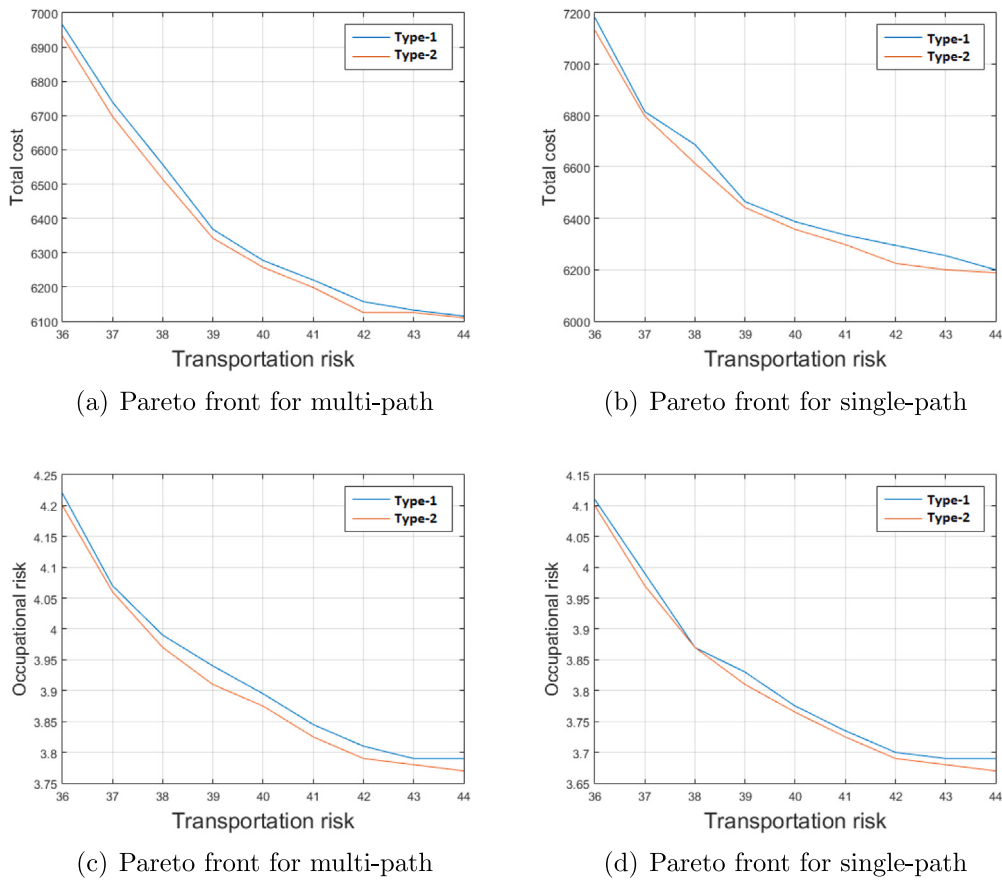


Fig. 14. Pareto front using Type-1 and Type-2 fuzzy logic.

**Table 14**

Computational time (seconds) for all models (using Type-1 and Type-2 fuzzy logic).

Models	Type-1		Type-2	
	(With multi-path)	(With single path)	(With multi-path)	(With single path)
Model A	237	278	317	381
Model B	122	135	122	135
	(NUFL)	(NUFL)	(NUFL)	(NUFL)
Model C	118	126	118	126
	(NUFL)	(NUFL)	(NUFL)	(NUFL)
Model D	497	559	577	662

NUFL: Not used fuzzy logic.

**Table 15**

Performance analysis using some performance indicators.

Instace	NDSTPF	Different Algo.	ONVG	OTNVG	OTNVGR (%)	DSTPF	ER	IGD	GD
Model D	84	SGA-I	51	36	70.58	15	0.29	781.12	103.82
		SGA-II	68	40	58.82	28	0.41	614.17	91.89
		SGA-III	62	48	77.41	14	0.22	314.25	83.54
		SGA-IV	74	63	85.13	11	0.14	94.47	38.46
		POBGA	81	74	91.35	7	0.08	0.17	5.29

NDSTPF: Non-dominated solutions in true Pareto-front, DSTPF: Dominated solutions in true Pareto-front.

other algorithms, POBGA performs better in terms of ER.

## 8. Managerial insight

This section outlines a comprehensive array of research questions and the corresponding managerial insights they offer. Mainly, this discussion focuses on the repercussions of COVID-19 on medical waste

routing, particularly concerning transportation logistics and occupational risks. Furthermore, the impact of factors such as multi-path routing and fixed charge costs is considered. To address this NP-hard real-life problem effectively, leveraging problem-specific crossover techniques and integrating partial oppositional-based Genetic Algorithms can be highly beneficial. We present the managerial decisions (to opt) out of the optimal results and their dissection in question-answer forms in Table 16. In developing countries like India, Bangladesh, and Sri Lanka, medical waste management poses a significant challenge,

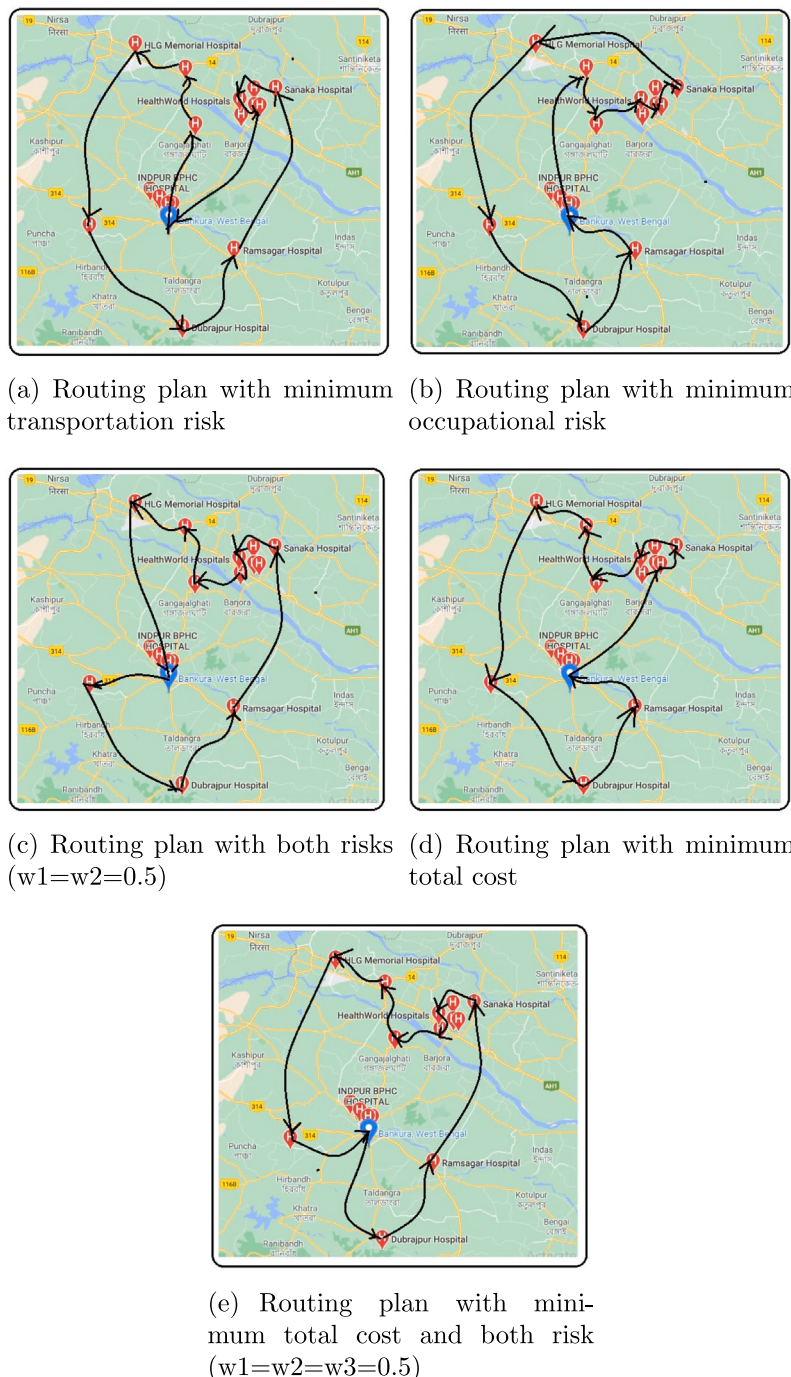


**Fig. 15.** Different routing plan for COVID-19 medical waste collection in Bankura district.

especially concerning hazardous COVID-19 medical waste. Although this investigation focuses on practical problems related to COVID-19 medical waste routing in the district of Bankura, West Bengal, India, encompassing 10 medical centers and the challenges associated with routing and handling hazardous medical waste, these methods can be readily implemented for other countries facing similar challenges with hazardous medical waste.

Management policies should address the occupational and transportation risks inherent in waste collection and transportation. To mitigate these risks, waste collectors should (i) receive training, (ii) adhere to regulations, (iii) take necessary precautions, and (iv) provide assistance to nearby individuals in the event of a road accident.

## 9. Conclusion and outlook

### 9.1. General comments

In MOMPC-19MWCP problems, we consider (i) Transportation risk (based on Type-2 fuzzy logic), (ii) Occupational risk, (iii) fixed cost (toll tax), (iv) loading cost for the items, (v) multi-path, (vi) traveling cost, (vii) weighted sum method based multi-objective solutions. Management can take the proper decision based on the real-life situation. To solve the above NP-hard type problems, a novel GA with (i) POBL-based initialization and mutation (ii) probabilistic selection, and (iii) weighted crossover are proposed and implemented successfully in some

**Table 16**  
Research questions, solutions and managerial insight.

Research Questions	Solutions (with reference)	Managerial insight
R1: What is the impact of COVID-19 medical waste routing problem?	Table 6, and Fig. 15	Management can take the appropriate decision for optimal routing plan
R2: How to address the transportation and occupational risks?	Tables 6, and 7	Two different risks are handled in these models.
R3: How to manage the risk limit in efficient manner?	Table 9, and Figs. 10(a), 10(b)	Considering different risk limits choose appropriate decision.
R4: What is the impact of multi-path in routing?	Tables 9, and 6	Management can take optimal decision for appropriate path selection.
R5: Why fixed charge cost is needed to be investigated?	Tables 6, and 7	Along different roads, fixed charges are collected, which can be handled through this models.
R6: How to manage, three objective into single one?	Table 10, and Section 3.7.4	Through weighted sum method take appropriate routing plan.
R7: Why problem specific is preferred?	Section 4.5, and Fig. 7	Through weighted crossover, crossover optimal solutions are generated faster.
R8: How does POBL based GA perform compared to the conventional GA?	Performances tested through statistical test. POBGA performs better than classical GA (Tables C.3–C.6)	Management can quickly solve the real-life routing models through POBGA.

MOMPC-19MWCP problems. This formulation can be used in the fields of another emergent routing, inventory control, supply-chain, etc., for better managerial decision-making. The developed MOMPC-19MWCP models can be modified and solved taking a specific country's present hazardous medical waste collection procedures into account. If the resources (availability of multiple medical vans) permit, the present problem can be formulated as a multiple vehicle routing problem and solved. The developed algorithm, POBGA, is in general form and can be applied in other TSP-type problems, such as the VRP, TPP, Facility location problem, Disaster management problem, etc.

## 9.2. Limitations

The limitations of our investigation are that (i) we consider the weighted sum method for multi-objective. It can be further solved through other multi-objective methods. (ii) only one vehicle is considered for collection (routing) due to resource constraints, (iii) the capacity of the vehicle is considered sufficient to accommodate all collected medical waste (The vehicle may be taken to have finite capacity), (iv) The investigation focuses solely on two input parameters for both Type-1 and Type-2 fuzzy logic. The addition of more input parameters would significantly increase computational time.

## 9.3. Future research scopes

In the future, (i) these models can be extended considering multi vehicles and multi compartment along with multi-path among the centers. (ii) These models can be readily implemented for other countries facing similar challenges with hazardous Covid-19 or others medical waste. (iii) MOMPC-19MWCP models with time windows can also be formulated and solved. (iv) Here POBL is used in initialization and mutation only. POBL can also be used in the selection and crossover for different versions of GA. POBL concept can also be used in other heuristic algorithms.

## CRediT authorship contribution statement

**Somnath Maji:** Writing – review & editing, Writing – original draft, Visualization, Validation, Software, Methodology, Data curation, Conceptualization. **Samir Maity:** Writing – original draft, Visualization, Supervision, Methodology, Conceptualization. **Debasis Giri:** Writing – original draft, Supervision. **Izabela Nielsen:** Writing – review & editing, Supervision. **Manoranjan Maiti:** Writing – review & editing, Validation, Supervision, Methodology, Conceptualization.

## Declaration of competing interest

The authors declare that they have no known competing financial interests or personal relationships that could have appeared to influence the work reported in this paper.

## Appendix A. Mathematical preliminaries

The concept of Type-2 fuzzy and Type-2 fuzzy logic are given below.

### A.1. Interval Type-2 fuzzy set (IT2FS) (cf. Castillo et al., 2007; Ullah et al., 2021)

A Type-2 fuzzy set (T2FS) expresses the nondeterministic truth degree with imprecision and uncertainty for an element that belongs to a set. A T2FS denoted by  $\tilde{A}$ , is characterized by a Type-2 membership function  $\mu_{\tilde{A}}(x, u)$ , where  $x \in X$ ,  $u \in J_x^u \subseteq [0, 1]$  and  $0 \leq \mu_{\tilde{A}}(x, u) \leq 1$  defined in Eq. (17) according to Mendel (2017) is given below

$$\tilde{A} = \{(x, \mu_{\tilde{A}}(x)) | x \in X\} = \{(x, \mu, \mu_{\tilde{A}}(x, u)) | \forall x \in X, \forall u \in J_x^u \subseteq [0, 1]\} \quad (17)$$

This is also expressed as

$$\tilde{A} = \int_{x \in X} \int_{\mu \in J_x^u} \mu_{\tilde{A}}(x, \mu) / (x, \mu) J_x^u \subseteq [0, 1] \quad (18)$$

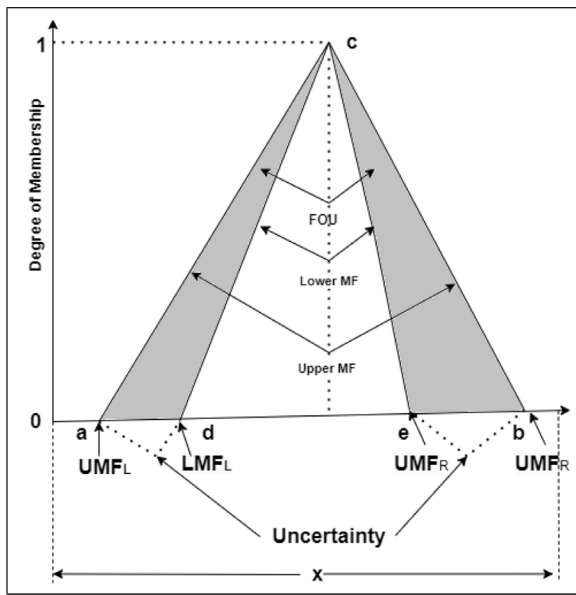


Fig. A.1. Type-2 fuzzy membership set.

Here,  $0 \leq \mu_{\tilde{A}}(x, u) \leq 1$ , and  $\int \int$  are the combination of given  $x$  and  $\mu$ .  $J_x$  indicates primary membership of  $\tilde{A}$  where  $J_x \subseteq [0, 1]$  for  $x \in X$ . From Eqs. (17), (18) and  $J_x \subseteq [0, 1]$  gives a restriction that is equivalent to  $0 \leq \mu_{\tilde{A}}(x, u) \leq 1$  for type-1 membership function (T1FSMF). For  $x = x'$ , and each value of  $x$ :

$$\mu_{\tilde{A}}(x') = \sum \mu \in J_{x'} f(x'/\mu) / \mu, \text{ for } \mu \in J_{x'} \subseteq [0, 1] \quad (19)$$

and  $x' \in x$

$$FOU(\tilde{A})(x') = \bigcup_{x \in X} J_x = (x, \mu) : \mu \in J_x \subseteq [0, 1] \quad (20)$$

According to the above Eqs. (19) and (20),  $J_{x'}$  and  $\mu_{\tilde{A}}(x')$  stated a primary and secondary membership functions of  $x$  and the together of all primary MFs denoted through the footprint of uncertainty (FOU). The T2FS contains two T1FS MF with bounds on  $FOU(\tilde{A})$ , a lower bound  $\underline{\mu}_{\tilde{A}}(x)$ , the upper bound  $\overline{\mu}_{\tilde{A}}(x)$ ,  $\forall x \in X$ . Now these are given below

$$\underline{\mu}_{\tilde{A}}(x') \equiv \overline{FOU(\tilde{A})} \mid \forall x \in X \quad (21)$$

and

$$\mu_{\tilde{A}}(x') \equiv \underline{FOU(\tilde{A})} \mid \forall x \in X \quad (22)$$

In interval T2FS

$$J_X = [\underline{\mu}_{\tilde{A}}(x), \overline{\mu}_{\tilde{A}}(x)], \forall x \in X \quad (23)$$

In the given Fig. A.1, showing that FOU (shaded region), lower MF (LMF) and upper MF (UMF) which are presented by five points ( $a, b, c, d, e$ ) and four linear functions. The centroid of T2FMF is formulated as

$$Triangular(x; a, b, c, d, e) = \max(0, \min(T_1, T_2, e))$$

$$\begin{aligned} UMF &= T_1(x; a, b, c) \\ LMF &= T_2(x; d, e, c) \\ c &= \frac{\sum_{i=1}^q \mu(x_i)x_i}{\sum_{i=1}^q \mu(x_i)} \end{aligned} \quad (24)$$

$$[c_1, c_2] = \left[ \frac{\sum_{i=1}^q \mu'(x_i)x_i}{\sum_{i=1}^q \mu'(x_i)}, \frac{\sum_{i=1}^q \mu''(x_i)x_i}{\sum_{i=1}^q \mu''(x_i)} \right] \quad (25)$$

Here,  $\mu''(x_i)$  and  $\mu'(x_i)$  are the given values of UMF and LMF (see Eqs. (24) and (25)), which maximizes and minimizes the weighted average. The Type-2 fuzzy set can handle complex and higher-order uncertainty.

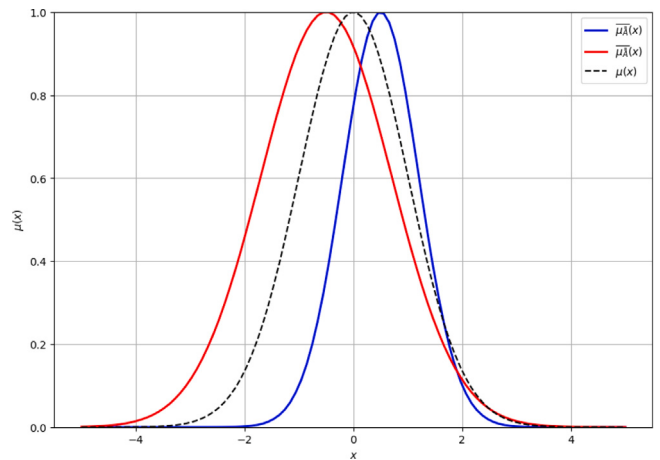


Fig. A.2. Upper, lower and mean membership for Type-1 fuzzy membership.

**Primary and secondary membership function:** For each  $x \in X$ , the primary membership  $J_x = [\underline{\mu}_{\tilde{A}}(x), \overline{\mu}_{\tilde{A}}(x)]$ , defines an interval of possible membership values. For a given  $x \in X$ , the secondary membership function  $\mu_{\tilde{A}}(x, u)$  can be represented as (in Eq. (26)):

$$\mu_{\tilde{A}}(x, u) = \begin{cases} f_x(u) & \text{if } u \in J_x, \\ 0 & \text{if } u \notin J_x, \end{cases} \quad (26)$$

where  $f_x(u)$  is the secondary membership function, usually a crisp value between 0 and 1. In interval Type-2 fuzzy sets (a special case of Type-2 fuzzy sets), the secondary membership function  $f_x(u)$  is equal to 1 for all  $u \in J_x$ . So, for the interval Type-2 fuzzy sets (in Eq. (27)):

$$\mu_{\tilde{A}}(x, u) = \begin{cases} 1 & \text{if } u \in J_x, \\ 0 & \text{if otherwise,} \end{cases} \quad (27)$$

Here, some examples of membership functions for Triangular Type-2 membership function (in Eq. (28)):

$$\mu_{\tilde{A}}(x, u) = \begin{cases} \frac{u - \underline{\mu}_{\tilde{A}}(x)}{\overline{\mu}_{\tilde{A}}(x) - \underline{\mu}_{\tilde{A}}(x)} & \text{if } u \in J_x, \\ 0 & \text{if otherwise,} \end{cases} \quad (28)$$

For Gaussian Type-2 membership function (in Eq. (29)):

$$\mu_{\tilde{A}}(x, u) = \exp \left( -\frac{(x - c)^2}{2\sigma^2} \right), \quad (29)$$

where  $c$  is the mean and  $\sigma$  is the standard deviation. Thus the upper membership functions (UMF) and lower membership functions (LMF) (a Fig. A.2) for that such as (in Eqs. (30) and (31)):

$$\overline{\mu}_{\tilde{A}}(x) = \exp \left( -\frac{(x - c_{UMF})^2}{2\sigma_{UMF}^2} \right), \quad (30)$$

$$\underline{\mu}_{\tilde{A}}(x) = \exp \left( -\frac{(x - c_{LMF})^2}{2\sigma_{LMF}^2} \right), \quad (31)$$

The Trapezoidal membership functions are given as (in Eq. (32)):

$$\mu_{\tilde{A}}(x) = \begin{cases} 0, & x \leq a \\ \frac{x-a}{b-a}, & a < x \leq b \\ 1, & b < x \leq c \\ \frac{d-x}{d-c}, & c < x \leq d \\ 0, & x > d \end{cases} \quad (32)$$

This equation defines the membership function  $\mu_{\tilde{A}}(x)$  for a Trapezoidal Type-2 fuzzy set. Here,  $a, b, c$ , and  $d$  are the parameters that define the trapezoidal shape of the membership function.

**Table A.1**  
Computational time for Rules-3, Rules-5 and Rules-25 through Type-2 fuzzy logic.

Models		Rules-3		Rules-5		Rules-25	
		Time (s)	TR	Time (s)	TR	Time (s)	TR
Model A	T1FL	WSP	87	56.21	118	55.72	237
		WMP	99	48.78	139	46.15	278
	T2FL	WSP	96	53.46	147	49.32	317
		WMP	103	41.82	189	37.25	34.17
Model D	T1FL	WSP	182	54.88	318	54.19	497
		WMP	217	52.93	389	52.26	559
	T2FL	WSP	223	50.13	412	49.38	577
		WMP	249	46.82	437	46.17	662

WMP: with multi-path, WSP: with single path, TR: Transportation risk.

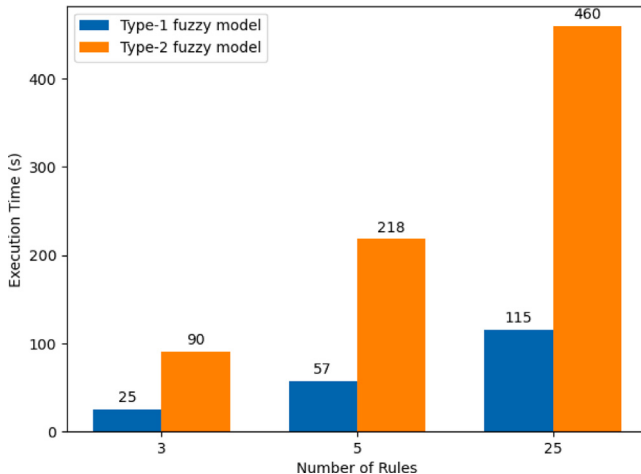


Fig. A.3. Rule vs. executions time in Type-1 and Type-2 fuzzy logic.

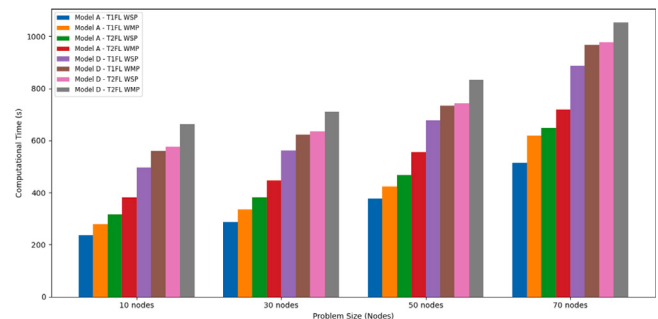


Fig. A.4. Nodes vs. executions time in Type-1 and Type-2 fuzzy logic.

optimal outcomes are achieved with 25 rules, despite the fact that this configuration requires more time.

### A.3. Type-2 fuzzy logic

The Mamdani IT2FIS ([Castro et al., 2007](#)) is designed with  $n$  inputs,  $m$  outputs, and  $r$  rules. The  $k$ th rule with interval Type-2 fuzzy antecedents  $\tilde{A}_{k,j} \in \{\mu_{i,l_{k,j}}\}$ , interval Type-2 fuzzy consequent  $\tilde{C}_{k,j} \in \{\sigma_{j,l_{k,j}}\}$  and interval Type-2 fuzzy facts  $\tilde{A}_i$  are inferred as a direct reasoning. The evaluation of this type of reasoning follows the formulation given by [Castillo et al. \(2007\)](#).

In this investigation, road specification data obtained by the IoT are crisp input in the T2FL. The crisps data are mapped by fuzzifier and sent to the T2FL rule to apply the “IF-THEN” rule. All the values of T2FS outputs are converted to T1FS outputs by type-reducer. Defuzzification further converts the T1FS onto a crisp value, which is approximately near the average of the right-end and left-end points (cf. [Fig. B.5](#)).

## Appendix B. Fuzzy system

### B.1. Assumptions/constraints regarding Fuzzy system

- (i) While numerous parameters contribute to road accidents, this investigation simplifies matters by focusing on two input parameters, namely road congestion and road surface, along with one output parameter, accident probability, both examined through Type-1 and Type-2 fuzzy logic. The addition of more input parameters would significantly increase computational time.
- (ii) The study utilizes historical records to obtain crisp values for input parameters. However, potential sudden environmental changes that could alter these values are not considered in this investigation.
- (iii) Another limitation lies in the challenge of effectively generating rules for arbitrary output parameters within a fuzzy rule-based system. This task can be particularly complex due to the intricate

**Table A.2**  
Computational time (seconds) for different problem sizes through Type-2 fuzzy logic.

Models		10 nodes	30 nodes	50 nodes	70 nodes
Model A	T1FL	WSP	237	286	377
		WMP	278	335	423
	T2FL	WSP	317	381	468
		WMP	381	446	556
Model D	T1FL	WSP	497	562	677
		WMP	559	623	735
	T2FL	WSP	577	635	742
		WMP	662	712	832

WMP: with multi-path, WSP: with single path.

### A.2. Computational complexity

Algorithmic complexity for Type-1 fuzzy models take lower than the Type-2 models. The computational complexity is typically  $\mathcal{O}(mn)$ , where  $m$  is the number of rules and  $n$  is the number of input variables. For Type-2 fuzzy models, the complexity increases due to the need to handle uncertainties in the membership functions, leading to a complexity of  $\mathcal{O}(mnk)$  where  $k$  represents the granularity level of the secondary membership functions. Both Type-1 and Type-2 fuzzy models for the present problem are implemented. The number of fuzzy rules and input variables is verified systematically. The [Fig. A.3](#) shows the different execution times for several inputs.

In [Tables A.1](#) and [A.2](#) (see, in [Figs. A.3](#) and [A.4](#)), results are derived by applying different sets of rules (rules-3, 5, 25) with varying numbers of nodes (nodes-10, 20, 50, 70). These results are then fine-tuned using Type-2 fuzzy parameters. It is observed that, across all cases, the

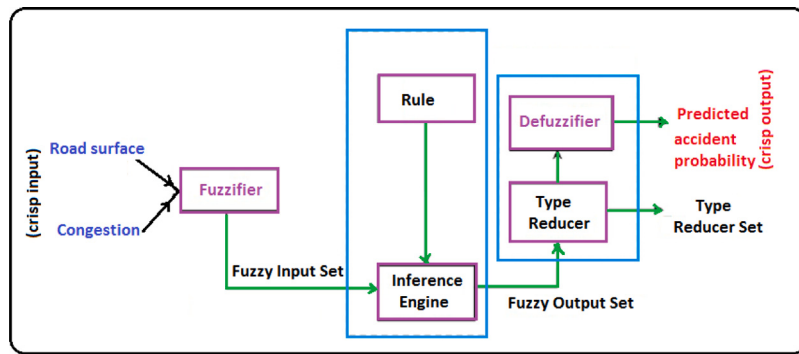


Fig. B.5. Block diagram of fuzzy system.

nature of mapping input variables to output parameters in a fuzzy logic framework.

- (iv) Type-1 and Type-2 fuzzy logic, each with 25 rules, were employed utilizing the Type-2 fuzzy logic toolbox (Castro et al., 2007). Although experimental iterations initially included 3 and 5 rules via the toolbox, superior outcomes were observed with the implementation of 25 rules.

In this fuzzy system, through gathering expert knowledge and reviewing relevant literature to determine the initial ranges and types of membership functions. These functions should align with the nature of the problem being modeled. Implement the Type-2 fuzzy model with the initial parameters and run simulations on a representative dataset. We have used a trial-run system for parameter tuning in the present Type-2 fuzzy model. Also, conduct a sensitivity analysis by systematically varying the fuzzy parameters and observing the impact on the model's results. This helps to identify the most critical parameters that significantly influence the output.

(i) Type = 'mamdani', (ii) Version = 2.0, (iii) NumInputs = 2, (iv) Numoutputs = 1, (v) NumRules = 25, (vi) AndMethod = 'min', (vii) OrMethod = 'max', (viii) ImpMethod = 'min', (ix) AggMethod = 'max', (x) DefuzzMethod = 'centroid',

#### Type-2 Fuzzy logic-based accident probability:

Fuzzy logic has been used for simulation. Road surface and Road congestion are taken as the inputs of the fuzzy controller. Rules are developed based on the conditions and requirements to make decisions as output.

In this model, to predict the accident probability, Type-1 and Type-2 fuzzy logic systems (Fig. B.5) are used. First, we use the input parameters of road surface and congestion for the Type-2 fuzzy logic system (Fig. B.11), and the crisp value of accident probability obtained as output using the fuzzy logic rules given in Table 3. The Fig. B.6 illustrates how expert opinions were utilized to estimate accident probabilities. Here, the opinions of three experts (yellow, blue, and black) were used to define the membership functions for a triangular fuzzy number. The right top side of the figure describes the outcome based on one expert's input. In Fig. B.6, the right bottom side depicts the footprint of uncertainty, as modeled using Type-2 fuzzy logic.

#### B.2. Rules for Type-1 and Type-2 fuzzy logic

For controlling the accident probability, we used 25 rules (Table 3), and the corresponding fuzzy linguistic values (Table 5) are given. Here, accident probabilities are evaluated using the rules and linguistic values for Type-1 and Type-2 fuzzy logic are presented in Figs. B.7 and B.8 respectively.

Here, the Figs. B.7, B.8, B.9, and B.11 are design using Type-2 fuzzy logic toolbox (Castro et al., 2007).

#### B.3. Fuzzy linguistics input/output values

Here, fuzzy linguistic values input data in (Table 5, Fig. B.9) and output data in (Table 5, Fig. B.11) are taken.

#### B.4. Accident probability by Type-1 and Type-2 fuzzy logic, and mathematical expression

##### B.4.1. Accident probability by Type-1 fuzzy logic

Using the rules and linguistic values, according to Table 5 and Fig. B.9 the accident probability is evaluated and presented in Fig. B.10.

Here, using the same set of rules for Type-1 fuzzy logic, it is observed that in a certain scenario, the accident probability becomes  $10^{-6.3}$  when Road surface and Road congestion are 0.5 and 0.67, respectively.

##### B.4.2. Accident probability by Type-2 fuzzy logic

The accident probabilities are evaluated using the rules and linguistic values for Type-2 fuzzy logic are presented in Table 5 and Fig. B.9.

Fig. B.11 illustrates various perspectives within Type-2 fuzzy logic. Figs. B.11(a) and B.11(b) represent the membership of Road surface and Road congestion respectively. Using the interval value viewer, for different values of Road surface and Road congestion, we get the corresponding accident probability from Fig. B.11(c). Using the same set of rules in the Type-2 fuzzy logic, it is shown that the accident probability becomes more dynamic in Fig. B.11(d).

This above process is numerically illustrated in Fig. B.12.

##### B.4.3. Accident probability by a mathematical expression

The accident probability can be expressed by a distribution function (in linear form) of two variables  $R_s$  and  $R_c$  given in Eq. (33):

$$\rho = A[|\log(R_s)| + |\log(1 - R_c)|] \quad (33)$$

where  $R_s$  and  $R_c$  represent the smoothness of road surface and degree of road congestion,  $R_s$  and  $R_c$  lie between (0,1,1) and (0,0,9) respectively.

If  $R_s=1$  then the road surface is very smooth, and hence the accident probability due to the road surface is 0 (as  $\log 1 = 0$ ). Similarly, if  $R_c = 0$ , i.e., the road is congested-free, and in this case, the accident probability is 0 (as  $\log(1 - R_c) = 0$ ). But in real-life,  $R_s$  cannot be 1; and similarly,  $R_c$  cannot be 0. Therefore, considering the actual case of the condition of road surface and congestion we assume that  $R_s$  and  $R_c$  lie within (0,1,1) and (0,0,9) respectively. Constant A is adjusted through practical observation.

Now taking  $R_s = 0.613$  and  $R_c = 0.476$  and  $A = (20/3) \times 10^{-7}$ , we get from Eq. (33),  $\rho = 3.2 \times 10^{-7}$ . Using Type-2 fuzzy logic from Fig. B.12,  $\rho = 10^{-6.58} = 2.63 \times 10^{-7}$ . It is observed that the probability of accidents ( $\rho$ ) is lower when using Type-2 fuzzy logic compared to the function given in Eq. (33).

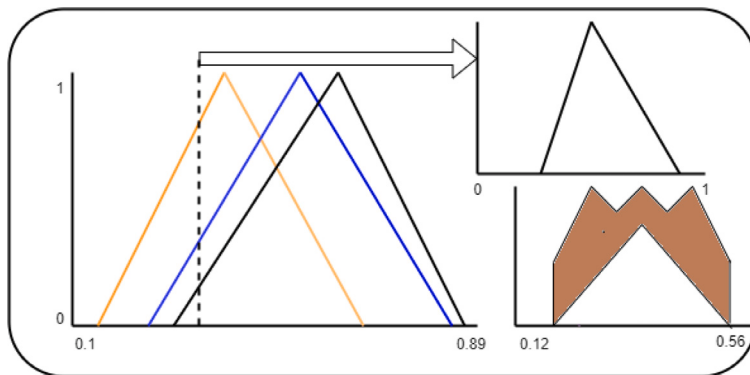


**Fig. B.6.** Accident probability for three expert using Type-2 fuzzy logic.

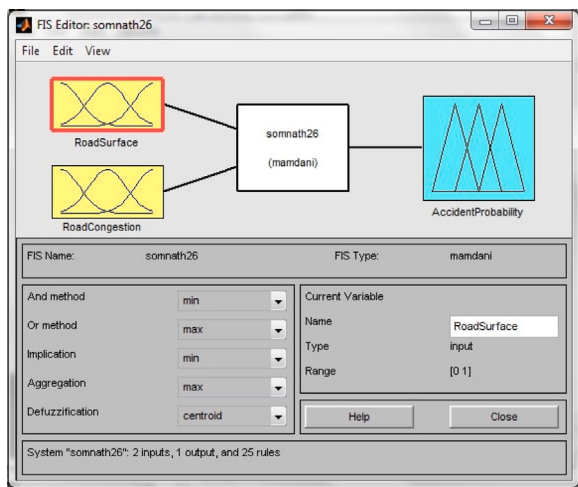


**Fig. B.7.** Accident probability by rules for Type-1 fuzzy logic.

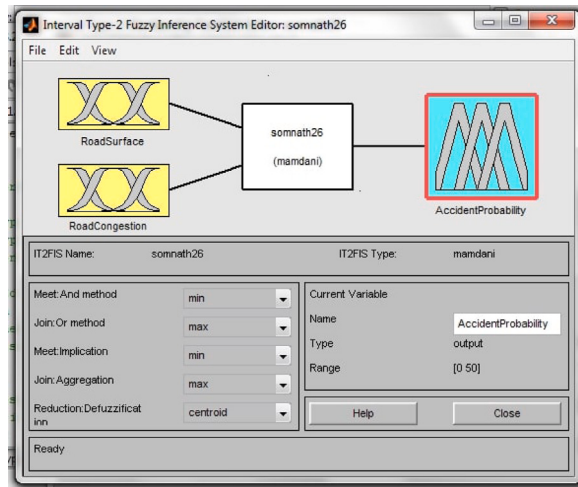


**Fig. B.8.** Accident probability by rules for Type-2 fuzzy logic.

The parameters like road congestion and surface quality are often described using linguistic terms. Fuzzy logic, which aligns well with these verbal descriptions, is generally expected to provide better results. Specifically, Type-2 fuzzy logic is more effective than Type-1 in managing the uncertainty and ambiguity of events, making it the preferred choice. Nevertheless, probability and fuzzy logic are two distinct

approaches, each suited to different applications, and comparing these systems is inherently difficult.

#### B.4.4. Evaluation of accident probability using Type-2 fuzzy logic with rules-3, 5 and 25

Here, the accident probability is determined using Type-2 fuzzy logic with different numbers of rules. In this investigation, we apply Type-2 fuzzy logic with rules 3 (Fig. B.14), 5 (Fig. B.13), and 25 (Fig. B.11). In all cases, the Type-2 fuzzy logic with rule 25 demonstrates superior performance.

### Appendix C. Performance of POBGA on TSPLIB problems

We used the standard TSP test data sets from TSPLIB (cf. Reinelt, 1995) to evaluate the efficiency and viability of the created algorithm POBGA. The results of the aforementioned classical TSP, using POBGA and ACO (Ant colony optimization), range from 16 to a maximum of 783 nodes, are reported in Table C.3. The overall cost, the number of iterations, and the CPU time in seconds are compared for these outcomes.

Regarding both solution quality and computational efficiency, POBGA surpassed ACO. The number of iterations the heuristic needs to make in order to find the best solution is shown in the *Iteration* column of Table C.3. For POBGA, we see substantially quicker convergence to the ideal solution, and its performance remains superior for larger instances.

#### C.1. Statistical test

To evaluate the effectiveness of the proposed algorithm in terms of solution quality, computational efficiency, and robustness to variations in problem instances we used the statistical test.

##### C.1.1. Dispersion against different test problems and different algorithms

Table C.4 provides the best known solution (BKS), average, and standard deviation (SD) of results from a certain heuristic over 8 instances on a specific benchmark test data set, as well as the error % of the best solution obtained from BKS. The benchmark data set's problem sizes range from 16 nodes to 101 nodes. In addition, we develop four variants of the standard GA methodology, called SGA-I (Roulette wheel selection, cyclic crossover, and random mutation), SGA-II (Rank selection, partial map crossover, and random mutation), SGA-III (Tournament selection, cyclic crossover, and random mutation), and SGA-IV (Probabilistic selection, cyclic crossover, and random mutation), to evaluate how well they perform in comparison to POBGA. In every instance, POBGA's average tour distance is less than the average results achieved by SGA-I, SGA-II, SGA-III, and SGA-IV. The SD highlights the algorithm's resilience by demonstrating that these methods are steady. We also determine which case has the lowest relative error

1. If (RoadSurface is VerySmooth) and (WeatherCondition is VeryVeryGood) then (AccidentProbability is C25) (1)
2. If (RoadSurface is VerySmooth) and (WeatherCondition is VeryGood) then (AccidentProbability is C24) (1)
3. If (RoadSurface is VerySmooth) and (WeatherCondition is Good) then (AccidentProbability is C23) (1)
4. If (RoadSurface is VerySmooth) and (WeatherCondition is Bad) then (AccidentProbability is C22) (1)
5. If (RoadSurface is VerySmooth) and (WeatherCondition is VeryBad) then (AccidentProbability is C21) (1)
6. If (RoadSurface is Smooth) and (WeatherCondition is VeryVeryGood) then (AccidentProbability is C20) (1)
7. If (RoadSurface is Smooth) and (WeatherCondition is VeryGood) then (AccidentProbability is C19) (1)
8. If (RoadSurface is Smooth) and (WeatherCondition is Good) then (AccidentProbability is C18) (1)
9. If (RoadSurface is Smooth) and (WeatherCondition is Bad) then (AccidentProbability is C17) (1)
10. If (RoadSurface is Smooth) and (WeatherCondition is VeryBad) then (AccidentProbability is C16) (1)
11. If (RoadSurface is Medium) and (WeatherCondition is VeryVeryGood) then (AccidentProbability is C15) (1)
12. If (RoadSurface is Medium) and (WeatherCondition is VeryGood) then (AccidentProbability is C14) (1)
13. If (RoadSurface is Medium) and (WeatherCondition is Good) then (AccidentProbability is C13) (1)
14. If (RoadSurface is Medium) and (WeatherCondition is Bad) then (AccidentProbability is C12) (1)
15. If (RoadSurface is Medium) and (WeatherCondition is VeryBad) then (AccidentProbability is C11) (1)
16. If (RoadSurface is Rough) and (WeatherCondition is VeryVeryGood) then (AccidentProbability is C10) (1)
17. If (RoadSurface is Rough) and (WeatherCondition is VeryGood) then (AccidentProbability is C9) (1)
18. If (RoadSurface is Rough) and (WeatherCondition is Good) then (AccidentProbability is C8) (1)
19. If (RoadSurface is Rough) and (WeatherCondition is Bad) then (AccidentProbability is C7) (1)
20. If (RoadSurface is VeryRough) and (WeatherCondition is VeryVeryGood) then (AccidentProbability is C6) (1)
21. If (RoadSurface is VeryRough) and (WeatherCondition is VeryGood) then (AccidentProbability is C4) (1)
22. If (RoadSurface is VeryRough) and (WeatherCondition is Good) then (AccidentProbability is C3) (1)
23. If (RoadSurface is VeryRough) and (WeatherCondition is Bad) then (AccidentProbability is C2) (1)
25. If (RoadSurface is VeryRough) and (WeatherCondition is VeryBad) then (AccidentProbability is C1) (1)

(a) 25 rules (1-11)

(b) 25 rules (12-25)

Fig. B.9. Rules for Type-2 fuzzy logic.

**Table C.3**  
Results for standard TSP problems (TSPLIB).

Instances	Best known solution (BKS)	POBGA			ACO		
		Cost (Rs.)	Iteration	Time (s)	Cost (Rs.)	Iteration	Time (s)
us16	6859	6859	52	0.05	6859	197	0.07
gr17	2085	2085	71	0.07	2085	289	0.13
gr21	2707	2707	156	0.11	2707	382	0.89
bays29	2020	2020	128	0.21	2020	411	1.81
eil51	426	426	402	0.62	426	646	2.08
st70	675	675	412	0.81	842	691	2.16
eil76	538	538	546	0.85	702	737	3.37
eil101	629	716	810	1.72	742	1012	3.81
kroA150	26 524	26 919	916	2.13	29 106	1122	4.12
kroB150	26 130	27 212	935	2.91	28 416	1247	4.30
a280	2579	3217	1227	3.14	3517	1492	5.92
lin318	42 029	44 814	1338	4.08	45 321	1537	6.14
pcb442	50 778	53 141	1516	5.42	59 614	1772	7.31
rat783	8806	10 212	1832	7.89	12 344	2235	9.12

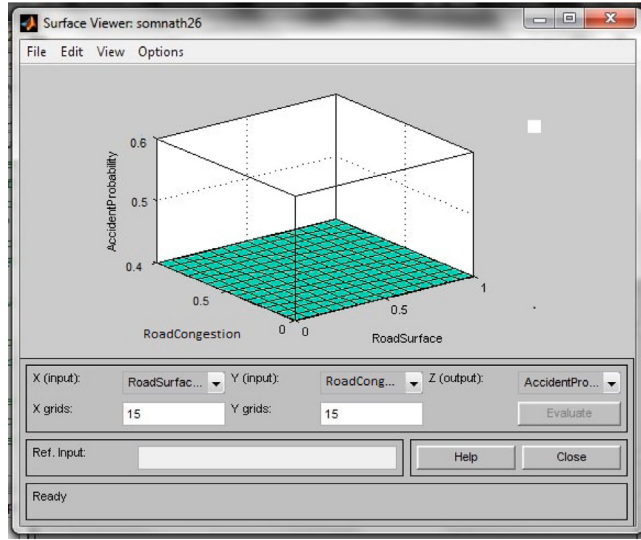


Fig. B.10. Surface view of accident probability by rules for Type-1 fuzzy logic.

percentage. These errors are also incredibly small, demonstrating how much closer to the BKS the generated average solutions are. As a result, the suggested POBGA has generated outcomes closer to ideal ones. Then, we run statistical analyses to determine how much POBGA's results differ from those of the other four GA-based methods.

#### C.1.2. Friedman's test

We perform the Friedman test (Derrac et al., 2011) to evaluate the performance of the algorithms SGA-I, SGA-II, SGA-III, SGA-IV, and POBGA. It is a non-parametric statistical method whose primary goal is to find a significant difference between the actions of two or more algorithms.

The assumptions of Friedman's test are as follows:

- The instances' (TSPLIB's) results stand alone from one another (i.e., the results within one instances does not influence the results within other instances).
- The observations (average objective values) for each case can be ranked.

In light of the valid assumptions, we create the following hypothesis:  
 $H_0$ : The likelihood of each algorithm ranking within each problem is equal (i.e., there is no difference between them).

$H_1$ : The average objective values for at least one of the algorithms are often higher than those for at least one of the other algorithms.

Considering the number of algorithms ( $k$ ) = 5 and the number of instances ( $b$ ) = 8, the Friedman ranking table (Table C.5) is prepared based on average values as reported in Table C.4.

Consider the expressions of  $A_2 = \sum_{i=1}^b \sum_{j=1}^k [R(X_{ij})]^2$ ,  $R_j = \sum_1^b R(X_{ij})$  for  $j = 1, 2, \dots, k$  and  $B_2 = \frac{1}{b} \sum_{j=1}^k R_j^2$ .

The test statistic is given by:  $T_2 = \frac{(b-1)[B_2 - b(k+1)^2/4]}{A_2 - B_2}$

From Table C.5, we calculate  $A_2 = 443$ ,  $B_2 = 431.75$  and the test statistic  $T_2 = 44.64$ . The respective F value with a significance level of  $\alpha = 0.01$  is  $F_{(1-\alpha), (k-1), (b-1)(k-1)} = F_{0.99, 4, 28} = 4.07$ . Since  $T_2 > F_{0.99, 4, 28}$ , we reject the null hypothesis. Hence, there exists an algorithm (POBGA), the performance of which is significantly different from the others.

#### C.1.3. (Post Hoc) paired comparisons

If the algorithms  $a$  and  $b$  are considered different after the rejection of the null hypothesis from Friedman's test, following the post hoc paired comparison technique (Derrac et al., 2011), we calculate the absolute differences of the summation of the ranks of algorithms  $a$  and  $b$  and declare  $a$  and  $b$  different if:

$$|R_a - R_b| > t_{1-\frac{\alpha}{2}} \left[ \frac{2b(A_2 - B_2)}{(b-1)(k-1)} \right]^{\frac{1}{2}}$$

where  $t_{1-\frac{\alpha}{2}}$  is the  $1-\frac{\alpha}{2}$  quantile of the t-distribution with  $(b-1)(k-1)$  degrees of freedom. Here,  $t_{1-\frac{\alpha}{2}}$  for  $\alpha = 0.01$  and 28 degrees of freedom is 2.76, and the critical value for the difference is = 17.74.

Table C.6 summarizes the paired comparisons, and the underlined values indicate the extent of differences between the algorithms. From

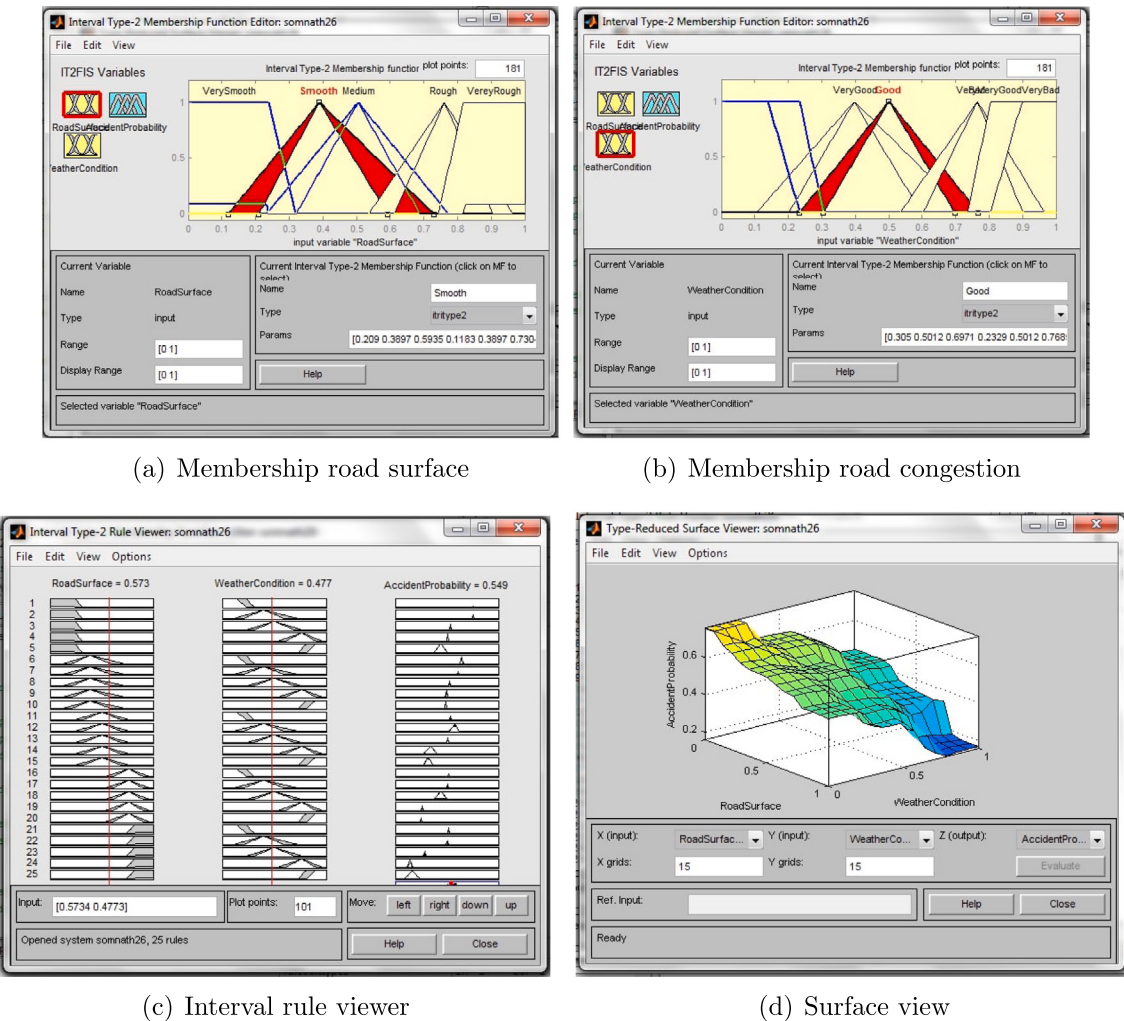


Fig. B.11. Graphical view of Type-2 fuzzy logic.

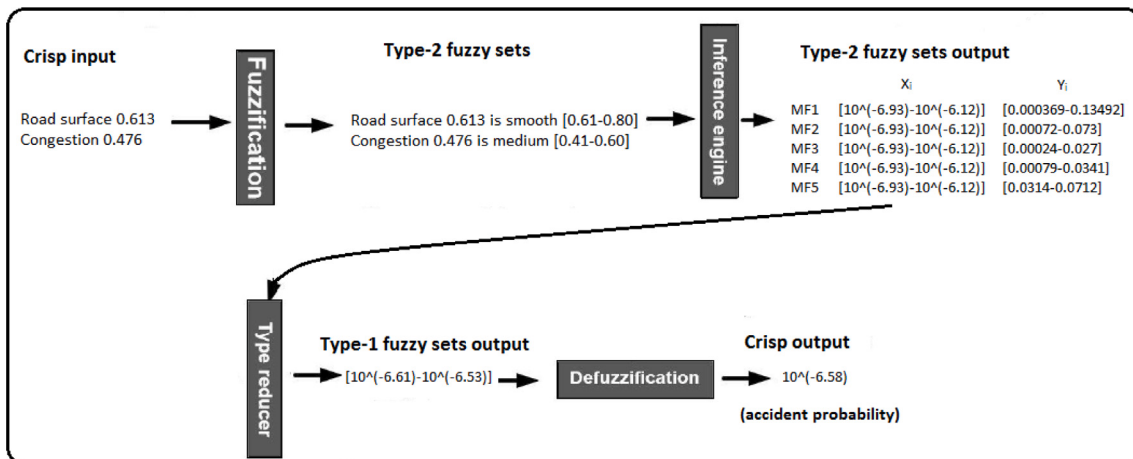


Fig. B.12. Example of Type-2 fuzzy logic.

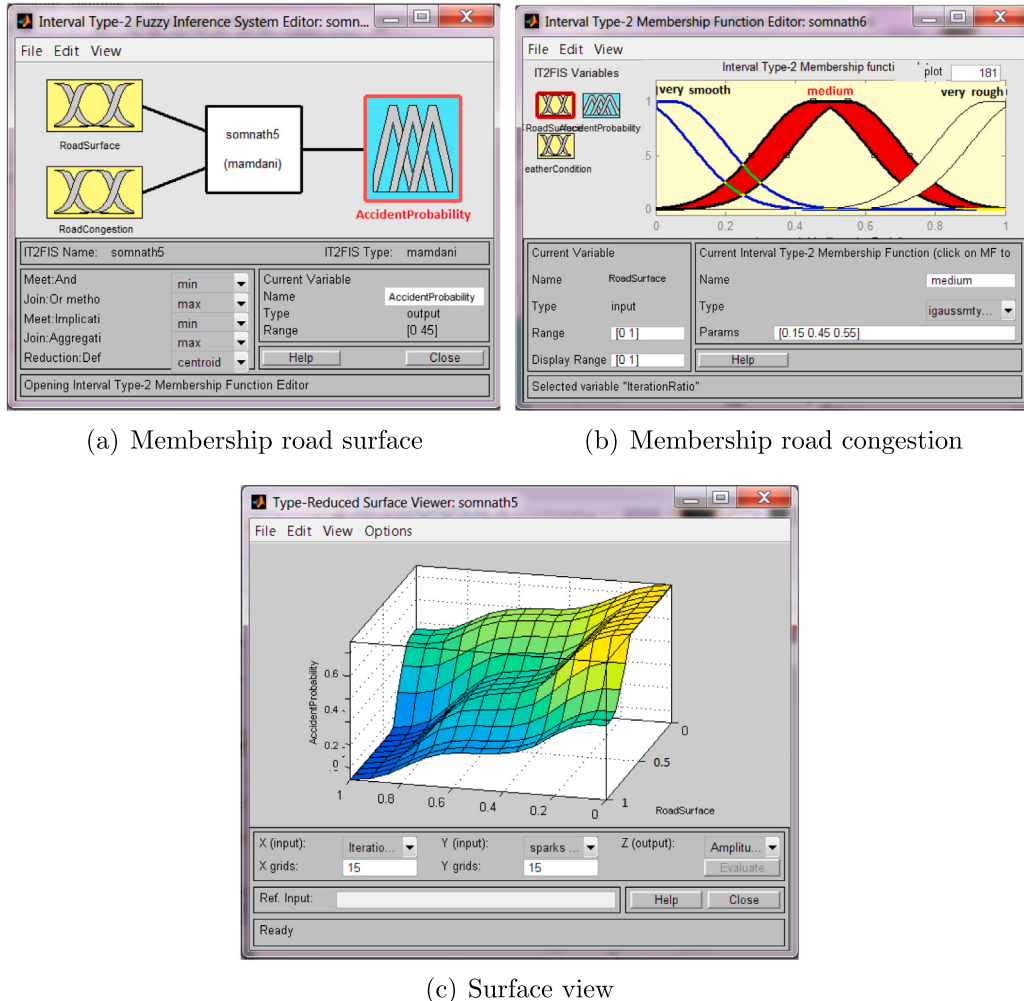


Fig. B.13. Graphical view of Type-2 fuzzy logic for rule 5.

**Table C.4**  
Results of POBGA and other methods.

Algorithm	Problem	us16	gr17	gr21	bays29	eil51	st70	eil76	eil101
SGA-I	BKS $\Rightarrow$	6859	2085	2707	2020	426	675	538	629
	Avg	7143.16	2211.23	2827.12	2152.92	597.17	1102.14	714.36	982.41
	SD	8.24	4.47	2.22	7.91	11.53	5.94	10.85	7.46
	Error (%)	4.01	5.94	3.92	6.24	39.96	57.38	31.52	55.17
SGA-II	Avg	6912.23	2114.13	2747.25	2137.12	527.27	899.31	699.29	927.67
	SD	2.92	3.22	1.74	4.96	6.57	4.81	6.24	5.36
	Error (%)	0.71	1.12	0.97	5.52	20.93	32.84	29.63	45.17
SGA-III	Avg	6882.13	2153.62	2781.17	2093.75	519.06	862.27	698.86	871.12
	SD	1.82	3.14	3.23	2.73	2.24	4.17	3.25	4.21
	Error (%)	0.31	3.11	2.52	3.53	20.17	26.43	28.94	37.83
SGA-IV	Avg	6991.18	2192.37	2796.22	2091.43	581.83	1041.42	699.83	952.14
	SD	4.71	2.60	5.63	2.21	4.21	3.91	3.99	6.23
	Error (%)	1.91	4.93	3.21	3.12	36.13	53.98	29.91	50.99
POBGA	Avg	6871.12	2095.89	2723.52	2031.24	452.23	731.93	624.76	713.17
	SD	0.91	0.82	0.51	1.62	1.93	2.72	2.31	3.62
	Error (%)	0.15	0.41	0.17	0.12	4.52	8.12	14.99	13.43

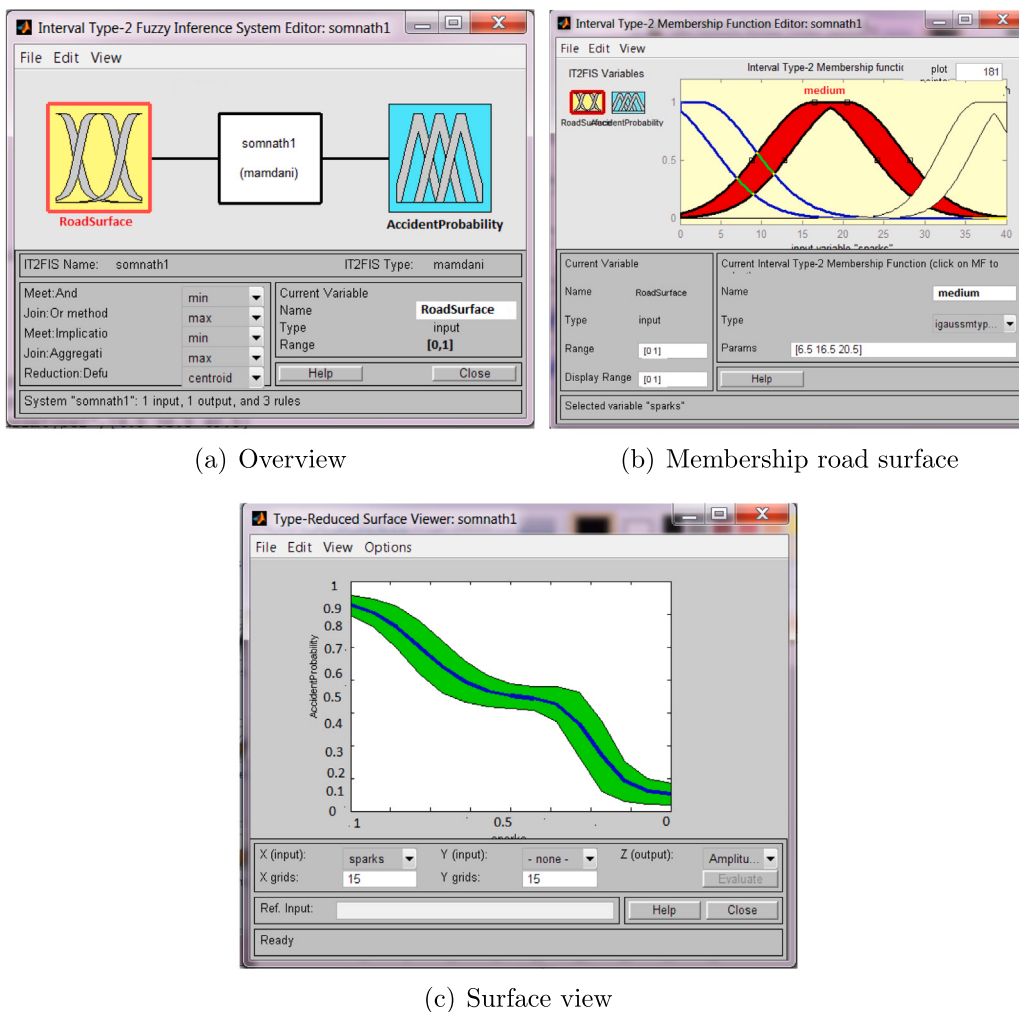


Fig. B.14. Graphical view of Type-2 fuzzy logic for rule 3.

**Table C.5**  
Ranking of Friedman's test.

Algorithms(k)	SGA-I	SGA-II	SGA-III	SGA-IV	POBGA
Instances(b)	R(X <sub>b1</sub> )	R(X <sub>b2</sub> )	R(X <sub>b3</sub> )	R(X <sub>b4</sub> )	R(X <sub>b5</sub> )
us16	5	3	2	4	1
gr17	5	2	3	4	1
gr21	5	2	3	4	1
bays29	5	4	3	2	1
eil51	5	3	2	4	1
eil70	5	3	2	4	1
eil76	5	3	2	4	1
eil101	5	3	2	4	1
Average rank	5	2.87	2.37	3.75	1
Summation	40	23	19	30	8

**Table C.6**  
Paired comparison of Friedman's test.

R <sub>i</sub> - R <sub>j</sub>	SGA-I	SGA-II	SGA-III	SGA-IV	POBGA
SGA-I	-	17	21	10	32
SGA-II	-	-	4	7	15
SGA-III	-	-	-	11	11
SGA-IV	-	-	-	-	22
POBGA	-	-	-	-	-

Table C.6, we conclude that POBGA has outperformed all of the other algorithms.

## Data availability

Data will be made available on request.

## References

- Al-Omran, K., Khan, E., Ali, N., Bilal, M., 2021. Estimation of COVID-19 generated medical waste in the Kingdom of Bahrain. *Sci. Total Environ.* 801, 149642.
- Alwabri, G., Al-Mikkhafi, A.S., Al-Hakimi, S.A., Dughish, M.A., 2017. Risk assessment of the current handling of medical waste in hospitals of Sana'a city Yemen. *Int. J. Sci. Technol.* 3 (1), 1–9.
- Castillo, O., Melin, P., Kacprzyk, J., Pedrycz, W., 2007. Type-2 fuzzy logic: Theory and applications. In: 2007 IEEE International Conference on Granular Computing. GRC 2007, IEEE, 145–145.
- Castro, J.R., Castillo, O., Martinez, L.G., 2007. Interval type-2 fuzzy logic toolbox. *Eng. Lett.* 15 (1), 89–98.
- Choi, M.J., Lee, S.H., 2011. The multiple traveling purchaser problem for maximizing system's reliability with budget constraints. *Expert Syst. Appl.* 38 (8), 9848–9853.
- Das, A.K., Islam, M.N., Billah, M.M., Sarker, A., 2021. COVID-19 pandemic and healthcare solid waste management strategy—a mini-review. *Sci. Total Environ.* 778, 146220.
- Derrac, J., García, S., Molina, D., Herrera, F., 2011. A practical tutorial on the use of nonparametric statistical tests as a methodology for comparing evolutionary and swarm intelligence algorithms. *Swarm Evol. Comput.* 1 (1), 3–18.
- Eren, E., Tuzkaya, U.R., 2021. Safe distance-based vehicle routing problem: Medical waste collection case study in COVID-19 pandemic. *Comput. Ind. Eng.* 157, 107328.

- Ergün, S., Usta, P., Alparslan Gök, S.Z., Weber, G.W., 2023. A game theoretical approach to emergency logistics planning in natural disasters. *Ann. Oper. Res.* 324 (1), 855–868.
- Fuertes, D., del Blanco, C.R., Jaureguizar, F., Navarro, J.J., García, N., 2023. Solving routing problems for multiple cooperative unmanned aerial vehicles using transformer networks. *Eng. Appl. Artif. Intell.* 122, 106085.
- Govindan, K., Nasr, A.K., Mostafazadeh, P., Mina, H., 2021. Medical waste management during coronavirus disease 2019 (COVID-19) outbreak: A mathematical programming model. *Comput. Ind. Eng.* 162, 107668.
- Gupta, S., 2022. Enhanced sine cosine algorithm with crossover: A comparative study and empirical analysis. *Expert Syst. Appl.* 198, 116856.
- Güvez, H., Muhammet, D., Tamer, E., 2012. Medical waste collection with vehicle routing problem in Kirikkale. *Int. J. Eng. Res. Dev.* 4 (1), 41–45.
- Hajar, Z., Btissam, D., Mohamed, R., 2018. Onsite medical waste multi-objective vehicle routing problem with time windows. In: 2018 4th International Conference on Logistics Operations Management. GOL, IEEE, pp. 1–5.
- He, Z.-g., Li, Q., Fang, J., 2016. The solutions and recommendations for logistics problems in the collection of medical waste in China. *Procedia Environ. Sci.* 31, 447–456.
- He, Z.G., Liu, S., 2015. The research on recovery network optimization of medical waste. In: Applied Mechanics and Materials. 768, Trans Tech Publ, pp. 671–678.
- Hirsch, W., Dantzig, G., 1968. The fixed charge transportation problem. *Nav. Res. Logist. Q.* 15, 413–424.
- Hu, Z., Bao, Y., Xiong, T., 2014. Partial opposition-based adaptive differential evolution algorithms: Evaluation on the CEC 2014 benchmark set for real-parameter optimization. In: 2014 IEEE Congress on Evolutionary Computation. CEC, IEEE, pp. 2259–2265.
- Jingwei, Z., Zujun, M., 2010. Fuzzy multi-objective location-routing-inventory problem in recycling infectious medical waste. In: 2010 International Conference on E-Business and E-Government. IEEE, pp. 4069–4073.
- Kargar, S., Pourmehdi, M., Paydar, M.M., 2020. Reverse logistics network design for medical waste management in the epidemic outbreak of the novel coronavirus (COVID-19). *Sci. Total Environ.* 746, 141183.
- Kim, I.Y., De Weck, O., 2006. Adaptive weighted sum method for multiobjective optimization: A new method for Pareto front generation. *Struct. Multidiscip. Optim.* 31 (2), 105–116.
- Koc, I., Cay, T., Babaoglu, I., 2022. A novel metaheuristic algorithm by efficient crossover operator for land readjustment. *Expert Syst. Appl.* 188, 116082.
- Koohestani, B., 2020. A crossover operator for improving the efficiency of permutation-based genetic algorithms. *Expert Syst. Appl.* 151, 113381.
- Kulkarni, B.N., Anantharama, V., 2020. Repercussions of COVID-19 pandemic on municipal solid waste management: Challenges and opportunities. *Sci. Total Environ.* 743, 140693.
- Li, Y., Hong, H., Sun, C., Geng, Z., Zhang, C., 2022. Collection and transportation system construction of potentially viral municipal solid waste during the COVID-19 pandemic in China. *Sci. Total Environ.* 157964.
- Liu, Z., Li, Z., Chen, W., Zhao, Y., Yue, H., Wu, Z., 2020. Path optimization of medical waste transport routes in the emergent public health event of covid-19: A hybrid optimization algorithm based on the immune-ant colony algorithm. *Int. J. Environ. Res. Public Health* 17 (16), 5831.
- Mahyari, K.F., Sun, Q., Klemes, J.J., Aghbashlo, M., Tabatabaei, M., Khoshnevisan, B., Birkved, M., 2022. To what extent waste management strategies need adaptation to post-COVID-19. *Sci. Total Environ.* 155829.
- Maity, S., Roy, A., Maiti, M., 2015. A modified genetic algorithm for solving uncertain constrained solid travelling salesmen problems. *Comput. Ind. Eng.* 83, 273–296.
- Maji, S., Maity, S., Bsau, S., Giri, D., Maiti, M., 2024. Varied offspring memetic algorithm with three parents for a realistic synchronized goods delivery and service problem. *Soft Comput.* 28 (5), 4235–4265.
- Maji, S., Maity, S., Castillo, O., Maiti, M., 2023a. A multi-path delivery system with random refusal against online booking using type-2 fuzzy logic-based fireworks algorithm. *Decis. Anal. J.* 6, 100151.
- Maji, S., Pradhan, K., Maity, S., Nielsen, I.E., Giri, D., Maiti, M., 2023b. Emergent multipath COVID-19 specimen collection problem with green corridor through variable length GA. *Expert Syst. Appl.* 232, 120879.
- Maji, S., Pradhan, K., Maity, S., Nielsen, I.E., Giri, D., Maiti, M., 2023c. Multipath traveling purchaser problem with time-dependent market structure using quantum-inspired variable length genetic algorithm. *Comput. Ind. Eng.* 186, 109710.
- Mendel, J.M., 2017. Uncertain rule-based fuzzy systems. In: Introduction and New Directions. vol. 684, Springer.
- Mete, S., Serin, F., 2019. Optimization of medical waste routing problem: The case of TRB1 region in Turkey. *Int. J. Optim. Control: Theor. Appl.* 9 (2), 197–207.
- Mosallanezhad, B., Gholian-Jouybari, F., Cárdenas-Barrón, L.E., Hajighaei-Kesheli, M., 2023. The IoT-enabled sustainable reverse supply chain for COVID-19 pandemic wastes (CPW). *Eng. Appl. Artif. Intell.* 120, 105903.
- Moustafa, A., Abdelhalim, A., Eltawil, A., Fors, N., 2013. Waste collection vehicle routing problem: Case study in Alexandria, Egypt. In: The 19th International Conference on Industrial Engineering and Engineering Management. Springer, pp. 935–944.
- Nabavi-Peleesarai, A., Mohammadkashi, N., Naderloo, L., Abbasi, M., Chau, K.-w., 2022. Principal of environmental life cycle assessment for medical waste during COVID-19 outbreak to support sustainable development goals. *Sci. Total Environ.* 827, 154416.
- Nolz, P.C., Absi, N., Feillet, D., 2011. Optimization of infectious medical waste collection using RFID. In: International Conference on Computational Logistics. Springer, pp. 86–100.
- Nolz, P.C., Absi, N., Feillet, D., 2014. A stochastic inventory routing problem for infectious medical waste collection. *Networks* 63 (1), 82–95.
- Oladzad-Abbasabady, N., Tavakkoli-Moghaddam, R., Mohammadi, M., Vahedi-Nouri, B., 2023. A bi-objective home care routing and scheduling problem considering patient preference and soft temporal dependency constraints. *Eng. Appl. Artif. Intell.* 119, 105829.
- Olatayo, K.I., Mativenga, P.T., Marnewick, A.L., 2021. COVID-19 PPE plastic material flows and waste management: Quantification and implications for South Africa. *Sci. Total Environ.* 790, 148190.
- Peng, D., Ye, C., Wan, M., 2022. A multi-objective improved novel discrete particle swarm optimization for emergency resource center location problem. *Eng. Appl. Artif. Intell.* 111, 104725.
- Reinelt, G., 1995. TSPLIB. <http://www.iwr.uni-heidelberg.de/groups/comopt/software>.
- Rubab, S., Khan, M.M., Uddin, F., Abbas Bangash, Y., Taqvi, S.A.A., 2022. A study on AI-based waste management strategies for the COVID-19 pandemic. *ChemBioEng. Rev.* 9 (2), 212–226.
- Saxena, A., 2019. A comprehensive study of chaos embedded bridging mechanisms and crossover operators for grasshopper optimisation algorithm. *Expert Syst. Appl.* 132, 166–188.
- Shang, C., Ma, L., Liu, Y., 2023. Green location routing problem with flexible multi-compartment for source-separated waste: A Q-learning and multi-strategy-based hyper-heuristic algorithm. *Eng. Appl. Artif. Intell.* 121, 105954.
- Si, T., Dutta, R., 2019. Partial opposition-based particle swarm optimizer in artificial neural network training for medical data classification. *Int. J. Inf. Technol. Decis. Mak.* 18 (05), 1717–1750.
- Si, T., Miranda, P.B., Bhattacharya, D., 2022. Novel enhanced Salp Swarm algorithms using opposition-based learning schemes for global optimization problems. *Expert Syst. Appl.* 207, 117961.
- Tam, N.T., Hoang, V.D., Binh, H.T.T., et al., 2022. Multi-objective teaching-learning evolutionary algorithm for enhancing sensor network coverage and lifetime. *Eng. Appl. Artif. Intell.* 108, 104554.
- Tang, J., Liu, X., Wang, W., 2023. COVID-19 medical waste transportation risk evaluation integrating type-2 fuzzy total interpretive structural modeling and Bayesian network. *Expert Syst. Appl.* 213, 118885.
- Taslimi, M., Batta, R., Kwon, C., 2017. A comprehensive modeling framework for hazmat network design, hazmat response team location, and equity of risk. *Comput. Oper. Res.* 79, 119–130.
- Taslimi, M., Batta, R., Kwon, C., 2020. Medical waste collection considering transportation and storage risk. *Comput. Oper. Res.* 120, 104966.
- Tirkolaei, E.B., Abbasian, P., Weber, G.-W., 2021. Sustainable fuzzy multi-trip location-routing problem for medical waste management during the COVID-19 outbreak. *Sci. Total Environ.* 756, 143607.
- Tizhoosh, H.R., 2005. Opposition-based learning: a new scheme for machine intelligence. In: International Conference on Computational Intelligence for Modelling, Control and Automation and International Conference on Intelligent Agents, Web Technologies and Internet Commerce. vol. 1, IEEE, pp. 695–701.
- Tsai, W.-T., 2021. Analysis of medical waste management and impact analysis of COVID-19 on its generation in Taiwan. *Waste Manag. Res.* 39 (1\_suppl), 27–33.
- Ullah, I., Youn, H.Y., Han, Y.-H., 2021. Integration of type-2 fuzzy logic and Dempster-Shafer theory for accurate inference of IoT-based health-care system. *Future Gener. Comput. Syst.* 124, 369–380.
- Voß, S., 1996. Dynamic tabu search strategies for the traveling purchaser problem. *Ann. Oper. Res.* 63 (2), 253–275.
- Wan, M., Ye, C., Peng, D., 2023. Multi-period dynamic multi-objective emergency material distribution model under uncertain demand. *Eng. Appl. Artif. Intell.* 117, 105530.
- Xu, Y., Yang, X., Yang, Z., Li, X., Wang, P., Ding, R., Liu, W., 2021. An enhanced differential evolution algorithm with a new oppositional-mutual learning strategy. *Neurocomputing* 435, 162–175.
- Yu, H., Sun, X., Solvang, W.D., Zhao, X., 2020. Reverse logistics network design for effective management of medical waste in epidemic outbreaks: Insights from the coronavirus disease 2019 (COVID-19) outbreak in Wuhan (China). *Int. J. Environ. Res. Public Health* 17 (5), 1770.
- Zhou, B., Bian, J., 2022. Multi-mechanism-based modified bi-objective Harris Hawks optimization for sustainable robotic disassembly line balancing problems. *Eng. Appl. Artif. Intell.* 116, 105479.